Interpretations of the performance of the Hybrid Extinction Retrieval Algorithms (HERA) during the CALIPSO Build 2 Tests

Stuart A. Young

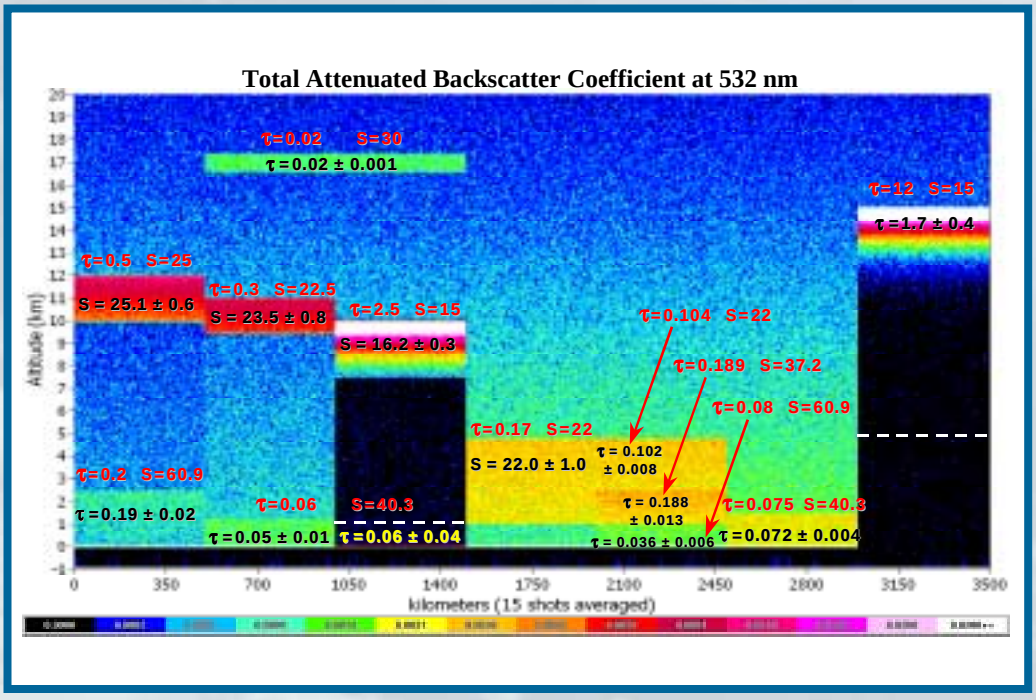

CSIRO Atmospheric Research

CSIRO Atmospheric Research Technical Paper 65

Interpretations of the Performance of the Hybrid Extinction Retrieval Algorithms (HERA) during the CALIPSO Build 2 Tests

Stuart A. Young

CSIRO Atmospheric Research Technical Paper No. 65

The National Library of Australia Cataloguing-in-Publication Entry

Young, Stuart A.
Interpretations of the performance of the hybrid extinction retrieval algorithms (HERA) during the CALIPSO Build 2 tests.

ISBN 0 643 06884 8.

1. Atmosphere - Remote sensing. 2. Optical radar. I. Title. (Series : CSIRO Atmospheric Research technical paper ; no. 65).

551.510287

Address and contact details: CSIRO Atmospheric Research
Private Bag No. 1, Aspendale Victoria 3195 Australia
Ph: (+61 3) 9239 4444; Fax: (+61 3) 9239 4400
Email: ar-enquiries@csiro.au

CSIRO Atmospheric Research Technical Papers may be issued out of sequence. From July 2000, all new Technical Papers will appear on the web site of CSIRO Atmospheric Research. Some Technical Papers will also appear in paper form.

Interpretations of the Performance of the Hybrid Extinction Retrieval Algorithms (HERA) during the CALIPSO Build 2 Tests.

Stuart A. Young,

CSIRO Atmospheric Research,
PMB 1 Aspendale VIC 3195,
Australia.

Abstract

The Hybrid Extinction Retrieval Algorithms (HERA) have been developed to perform data analysis tasks associated with the retrieval of particulate backscatter and extinction information from lidar data acquired during NASA's planned CALIPSO (Cloud-Aerosol Lidar and Infrared Pathfinder Satellite Observations) mission. The particular difficulties encountered in the automatic analysis of lidar data from space require the use of adaptive methods that select different analysis parameters autonomously according to the nature of the atmospheric target and quality of the lidar signal. The HERA software module is one of several closely-linked modules that form the CALIPSO lidar data analysis system. Because of the complexity of the algorithms, and of the interactions between the various software modules, a suite of simulated test cases has been developed to examine the performance of the HERA and other modules. The results of these tests of the second stage build of the analysis algorithms (the Build 2 tests) are the subject of this document.

In addition to providing tests of the accuracy of the HERA, the Build 2 tests provide insight as to the limits to the retrieval of useful information under a variety of atmospheric and signal conditions. These limits are discussed, as are suggestions for the improvement of the SIBYL (Selective Iterated BoundarY Locator) – HERA interface. Methods are also proposed that would improve the retrieval of information from the generally poorer quality 1064-nm lidar data.

1. Introduction

NASA's CALIPSO mission (Winker et al., 2002) will be launched in early 2005 to gather long-term, global data on the physical, optical and infrared properties of clouds and aerosols with the aim of significantly reducing the uncertainties in the predictions of global climate models. One of the instruments on board the CALIPSO satellite will be a two-wavelength, dual-polarization lidar that will provide profiles of particulate backscatter and extinction coefficient, and ancillary layer-integrated parameters, at 532-nm and 1064-nm. Several factors associated with satellite-based lidar measurements lead to difficulties not faced to the same degree in the analysis of data from ground-based lidar. These include the large distance of the lidar from the atmospheric target and the relatively low laser power. These factors mean that the single-shot lidar signal will usually have a low signal-to-noise ratio (SNR). Traditionally the SNR is improved by averaging many profiles. However, the relatively low laser firing rate, combined with the high speed of the satellite over the targets and the along-track variability of the targets, mean that it is not always possible to average a large number of profiles. The averaging of dissimilar profiles is not justified mathematically and leads to physically meaningless results. Methods have been devised whereby different altitude regions in a composite profile are produced by averaging different numbers of individual profiles and are analysed separately. The selective averaging and feature boundary location is

performed by the SIBYL algorithms (Vaughan et al., 2002), while the task of autonomously selecting the calibration and analysis parameters for the individual sections of profile is performed by the HERA module (Young, 2002; Young et al., 2002). The mathematical basis for the HERA analysis is presented in Young (2002), the structure and functions of the software modules described in Young (2001a) and results of initial tests on simulated data in Young (2001b).

The interaction between the HERA and SIBYL modules is complex and the performance of the HERA is strongly dependent on the correct interpretation of the data provided by the SIBYL. The possibilities for misinterpretation are numerous and the consequences vary from the subtle to the obvious. In order to test the accurate performance of the HERA and the correct operation of the interface between the SIBYL and the HERA, a suite of simulated lidar signals was created. The results of the tests of the performance of this second stage build of the analysis software (the Build 2 tests) are the subject of this paper.

The various test data scenes are described in Section 2, and the results of the tests in Section 3. Section 4 includes a discussion of the results and suggestions for overcoming some of the difficulties encountered on the tests. The Conclusions section includes initial conclusions on the limits to which useful retrievals can be obtained and a summary of recommendations in areas where the algorithms are still under development.

2. The Build 2 tests

A major aim of the Build 2 tests was to test the accuracy of the HERA retrievals. Systematic errors, mathematical or software coding errors would be identified, as would errors in the SIBYL – HERA data interface. The method was to generate several test files that simulated the lidar signal from different types of atmospheric "scenes" after initial processing by the SIBYL. The files were then analysed by the HERA and the outputs compared with the known simulation parameters. As the simulated signals included simulated instrumental noise and noise arising from illumination of the target by the sun or moon, interpretation of the results considered the statistics of the retrieved parameters.

Four different types of atmospheric feature were simulated. These were (a) lofted layers in which the optical thickness could be determined using the transmittance method as described by Young (1995), (b) lofted layers in which the optical thickness was too small to measure accurately, (c) layers in contact with the surface, and (d) layers in which the lidar signal was attenuated completely. For the analysis of the lofted layers with measurable optical thickness ($\tau > 0.1$) the SIBYL supplied the transmittance value to the HERA, which was then required to retrieve the mean lidar ratio for the layer. For the other cases, where the SIBYL could not determine the layer transmittance, the lidar ratio was supplied and the optical thickness was retrieved. In all cases, the HERA was also required to retrieve profiles of particulate backscatter and extinction at both 532 nm and 1064 nm, and the weighted mean ratio of the backscatter at the two wavelengths calculated through the depth of the feature. For the Phase 1 testing, the SIBYL supplied the correct values of the lidar ratio, transmittance and layer boundary parameters to the HERA, so as to focus the tests, as much as possible, on the performance of the HERA. For the testing in Phase 2, the SIBYL and HERA modules were joined and the parameters supplied to the HERA were subject to the uncertainties in their estimation by the SIBYL. (For a complete description of the Build 2 tests see Anselmo et al. (2002).)

Fourteen different atmospheric scenes were simulated. Each scene contained a combination of the atmospheric features described above. In the even-numbered simulations, the noise levels and instrumental settings represented those typical of nighttime operations. The odd-numbered simulations were identical except that daytime noise and settings were simulated. The seven simulated nighttime scenes are plotted side-by-side on height versus distance axes in Figure 1. Each scene except the last (212/213) contains a simulated boundary layer aerosol; scenes 202 and 204 contain a layer of "sub-visible" cirrus with an optical thickness of 0.02 that is below the SIBYL 5-km averaging threshold, while scenes 200, 202 and 204 contain a cirrus layer with an optical thickness that is measurable by the SIBYL. Scenes 212/213 contain a cloud that attenuates the lidar signal completely ($\tau = 12$). The aerosol layer in scene 206/207 is lofted above the surface. Scenes 208/209 contain three vertically adjacent aerosol layers of dissimilar properties.

3. Results

The results of the Phase 1 tests are presented in tabular form in Appendix A. For each simulation case, the results are presented for each feature and for each horizontal averaging grid used by the SIBYL to detect the feature. For example, in test case 204A a strong cirrus feature was detected and analysed after averaging to 5-km horizontal resolution, a weaker cirrus feature was detected after averaging to 20-km horizontal resolution, while the boundary-layer aerosol feature was only detected after averaging over 80-km. However, in test case 202 a strong cirrus feature was detected at 5-km resolution, while both the weaker cirrus feature between 16.5 km and 17.4 km altitude and the boundary layer aerosol were detected at 20-km horizontal resolution, so there were no remaining features to be detected at 80-km resolution. Each test case covers 480 km, so averages at 5, 20 and 80 km resolution contain 96, 24 or 6 samples respectively.

The quantities listed in the tables are the lidar ratio, the particulate optical thickness (depth), the mean particulate extinction coefficient, the mean particulate backscatter coefficient, the mean of the ratio of the backscatter at 1064 nm to that at 532 nm, and the vertical and horizontal standard deviations in the retrieved extinction coefficient. The tables list the minimum, maximum, mean, standard deviation and target values for each parameter at both 532 nm and 1064 nm.

To illustrate the manner in which the results are reported, consider, for example, the results of the analysis of test case 200. (See Appendix A, Table A1.) For the feature between 9.975 and 12.015 km, the optical thickness at 532 nm ($\tau = 0.5$) was supplied, so the standard deviation is reported as zero. The retrieved quantity in this case was the lidar ratio. A mean of 25.1 with a standard deviation of 0.6 compares well with the target value of 25 sr. At 1064 nm, however, it is not possible to measure the optical thickness so the lidar ratio (25.0) was supplied and the optical thickness was retrieved with a mean of 0.490 and a standard deviation of 0.0096, compared with the target value of 0.50. The results of the tests are presented in Figure 1, where the retrieved parameters are printed in black (or yellow for case 204), compared with the target values in red.

4. Discussion of results

For reasons that will become apparent later, it is convenient to divide the discussion into consideration of the retrieval of the upper-most layers and of the lower layers. Discussion of cases 208/209 and 212/213 is deferred until later.

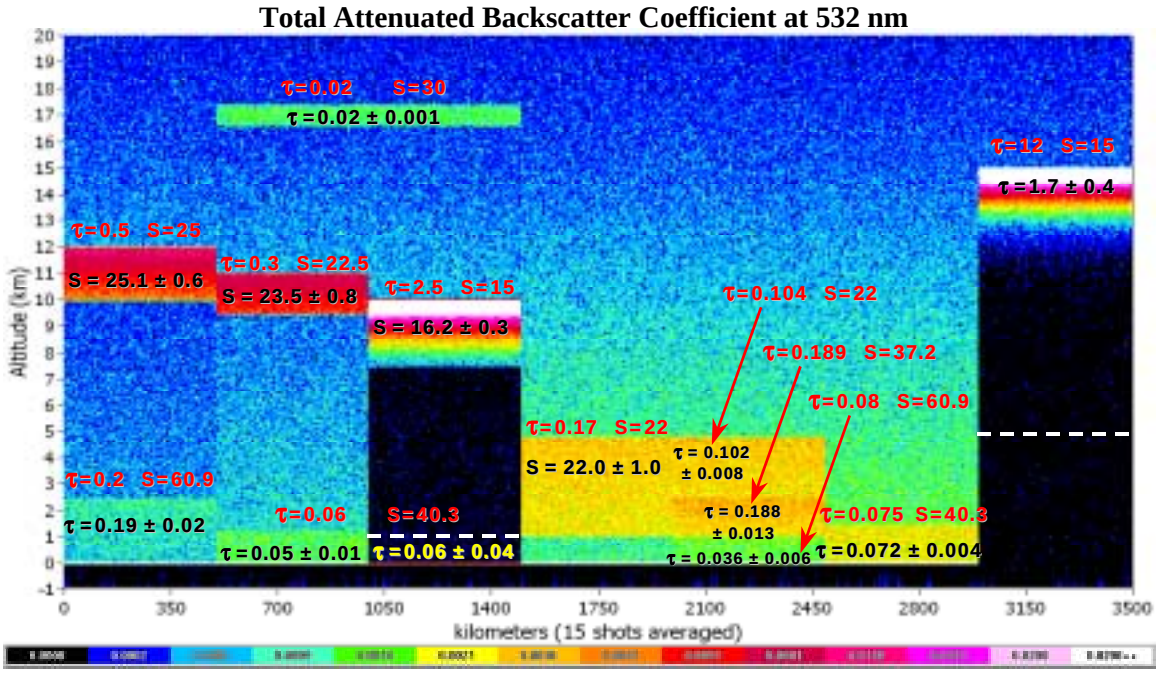

Figure 1: Simulated nighttime signals and retrieved parameters (in black) at 532 nm. (Adapted from Vaughan et al., 2002). The scenes are the even-numbered simulations 200-212. The dashed lines in simulations 204 and 212 indicate feature boundaries that are below the noise and digitization thresholds and cannot be plotted. The optical thickness is indicated by the τ values, while S is the simulated lidar ratio. Target values are shown in red, while retrieved values are shown in black (yellow for simulation 204). The colour scale units for the attenuated backscatter are $km^{-1}sr^{-1}$.

4.1 Upper-most features

As can be seen in the summaries in Appendix A, the retrieval of the parameters for the upper-most features is excellent. The retrieved parameters match the target values within the statistical uncertainties. Even at 1064 nm, where the signal is of poorer quality and has a lower SNR, the parameters are retrieved accurately, as can be seen in Table 1.

Table 1. Retrieved parameters at 1064 nm for the upper-most feature. (Adapted from Vaughan et al.,2002)

Scene	Base	Top	Type	Averaging	Lighting	τ_{target}	$\tau_{retrieved}$
200	9.975	12.015	Cloud	5-km	Night	0.500	0.490 ± 0.010
201	9.975	12.015	Cloud	5-km	Day	0.500	0.489 ± 0.015
202	16.575	17.415	Cloud	20-km	Night	0.020	0.019 ± 0.001
203	16.575	17.415	Cloud	80-km	Day	0.020	0.019 ± 0.001
204	16.575	17.415	Cloud	20-km	Night	0.020	0.020 ± 0.001
205	16.575	17.415	Cloud	20-km	Day	0.020	0.020 ± 0.002
206	0.990	4.800	Aerosol	5-km	Night	0.196	0.194 ± 0.009
207	0.990	4.800	Aerosol	20-km	Day	0.196	0.194 ± 0.006
208	2.490	4.800	Aerosol	5-km	Night	0.118	0.119 ± 0.005
209	2.490	4.800	Aerosol	5-km	Day	0.118	0.119 ± 0.005
210	0.030	1.500	Aerosol	20-km	Night	0.023	0.022 ± 0.002
211	0.030	1.500	Aerosol	80-km	Day	0.023	0.021 ± 0.001

4.2 Lower features

It can be seen from the tables in Appendix A and from Figure 1 that the retrieved parameters for some features below the upper-most feature are in error, and that the errors increase with the magnitude of the optical thickness of the overlying layers. This effect is particularly noticeable in the 1064-nm retrievals shown in Table 2.

The reason for the discrepancy between the target and retrieved parameters for the lower layers can be traced to different interpretations of the data interface between the SIBYL and HERA modules. The HERA module expects that the magnitude of the signal from altitude regions below a feature will be corrected for the attenuation caused by that feature. However, this correction is not always performed by the SIBYL module. Consider, for example, the 532-nm retrieval in case 202. The 10-km cirrus feature is detected by the SIBYL on the first pass processing where profiles are averaged to 5-km horizontal resolution. The attenuation of the cirrus layer is measured using the transmittance method (Young, 1995), and the signal from the underlying regions is rescaled to correct for this attenuation. However, the cirrus layer at 17 km is not detected until the second pass in SIBYL when profiles are averaged to 20-km horizontal resolution. Also, in this case, the optical thickness at 0.02 is below the detection threshold in the SIBYL. Underlying features are, therefore, not corrected for the attenuation of this layer, and are approximately four per cent lower than expected by the HERA. In particular, the cirrus feature detected at 10 km could not have been corrected for this attenuation on the previous pass, as the SIBYL was not aware of the existence of the upper layer at that stage. Also, SIBYL does not make a retrospective correction of the signals from previous passes for the attenuation of features detected in later passes when more averaging is used. Because the attenuated backscatter signal is too low, when the HERA adjusts the lidar ratio to bring the calculated optical thickness into agreement with the value supplied by the SIBYL as a solution constraint, the adjusted lidar ratio is too high in the same proportion. Note that the retrieved lidar ratio in this case is 23.45 ± 0.77 sr which, when scaled by the two-way attenuation of the 17-km cirrus layer (τ = 0.02), gives a corrected lidar ratio of 22.53 sr, which is in close agreement with the target value of 22.5 sr. This same effect biases the 1064-nm retrievals below undetected features. There are other effects at 1064-nm that will be covered below.

Table 2. Retrieved parameters at 1064 nm for lower features. (Adapted from Vaughan et al., 2002)

Scene	Base	Top	Type	Averaging	Lighting	τ_{target}	$\tau_{retrieved}$
200	0.030	2.490	Aerosol	20-km	Night	0.060	0.015 ± 0.004
201	0.030	2.490	Aerosol	80-km	Day	0.060	0.016 ± 0.002
202	9.495	10.995	Cloud	20-km	Night	0.300	0.276 ± 0.005
203	9.495	10.995	Cloud	20-km	Day	0.300	0.275 ± 0.007
204	0.030	1.200	Aerosol	80-km	Night	0.018	-0.003 ± 0.001
205	0.030	1.200	Aerosol	80-km	Day	0.018	-0.003 ± 0.002
208	0.990	2.490	Aerosol	5-km	Night	0.113	0.112 ± 0.006
209	0.990	2.490	Aerosol	20-km	Day	0.113	0.113 ± 0.007
208	0.030	0.990	Aerosol	20-km	Night	0.024	0.013 ± 0.002
209	0.030	0.990	Aerosol	80-km	Day	0.024	0.014 ± 0.002

4.3 Special Cases

Case 208 / 209

The scene in cases 208 and 209 is quite different from any of the others in that it contains two layers that partly overlap in height. The effect is to produce three adjacent layers of different optical properties. While the extinction algorithm correctly retrieved the parameters for the layers between 2.49 and 4.80 km and 0.99 and 2.49 km, the extinction coefficient through the lowest layer (0.030 to 0.99 km) was not retrieved accurately. The main reason is the one described above. That is that the profiles supplied to the HERA were not corrected for the attenuation of the overlying layers as expected. The second reason is that the extinction routines were unaware of the existence of another layer, detected at a finer averaging resolution that was in contact with the layer being analysed. This is because of the current SIBYL-HERA interface, where the extinction retrievals begin with the coarse resolution (80-km) profiles and work down to finest resolution. (The current retrieval algorithms are not yet capable of correctly analysing vertically-adjacent features that are detected at different horizontal resolutions.) The particulate extinction at the normalization height was, therefore, set to a default value of zero and the attenuation correction over the height increment between the normalization height and the first point in the layer was underestimated, thus leading to a retrieved extinction profile that was slightly too small. This is similar to the problem encountered with 1064-nm data discussed in the next section.

Case 212 / 213

The simulations in test cases 212 and 213 are of a cloud with a very high optical thickness (τ=12). As can be seen in Figure 2, the simulated attenuated backscatter signal (the green trace) is reduced to zero within about 4 km from the cloud top, well above the real cloud base at 5 km altitude. In order to digitize the signal correctly, the digitizer would need a dynamic range in excess of 11 orders of magnitude (~ 38 bits) - far in excess of the capability of the CALIPSO digitizer. The blue trace is the uncertainty in the attenuated backscatter and rises to 20 to 300% of the signal within 3 to 4 km below cloud top. (In a more realistic simulation, the SIBYL would most likely report an apparent cloud base between about 11.5 and 12 km.) It is thus not possible for the true optical thickness to be retrieved in this case. Note that although the retrieved extinction coefficient (the magenta trace with the uncertainty in violet) is on target at the top of the cloud, it starts to diverge once the retrieved optical depth exceeds about 1.5. As is well known, unconstrained forward solutions in cases of high optical thickness are unstable and very susceptible to errors in normalization, lidar ratio, the molecular model, and signal quality (SNR).

4.4 Other considerations for the analysis of 1064-nm data.

The most significant difference between the signals at 1064 nm and 532 nm is the lack of a measurable signal at the longer wavelength from the molecular atmosphere. This difference results from the fact that molecular scattering is inversely dependent on the wavelength of the scattered radiation raised to the fourth power. The molecular scattering at 1064 nm is thus one sixteenth of that at 532 nm. The scattering from clouds, however, is of similar magnitude at both wavelengths and the signal digitizer would, therefore, have to have a dynamic range that was over an order of magnitude greater at the longer wavelength in order to capture both cloud and molecular signals at similar resolution to measurements at 532 nm. There is also the additional problem that the background noise at 1064-nm is not one sixteenth of that at 532 nm, so the molecular signal, where it is strong enough to be measured, has a poor SNR. This

has several implications for the analysis of the 1064-nm data. The two most significant are that it is not possible to perform a normalization of the measured signal against the molecular model signal, and that it is not possible to use the transmittance method to determine the optical thickness of a feature. The consequence of this is that the extinction solutions cannot be constrained as they are at 532 nm.

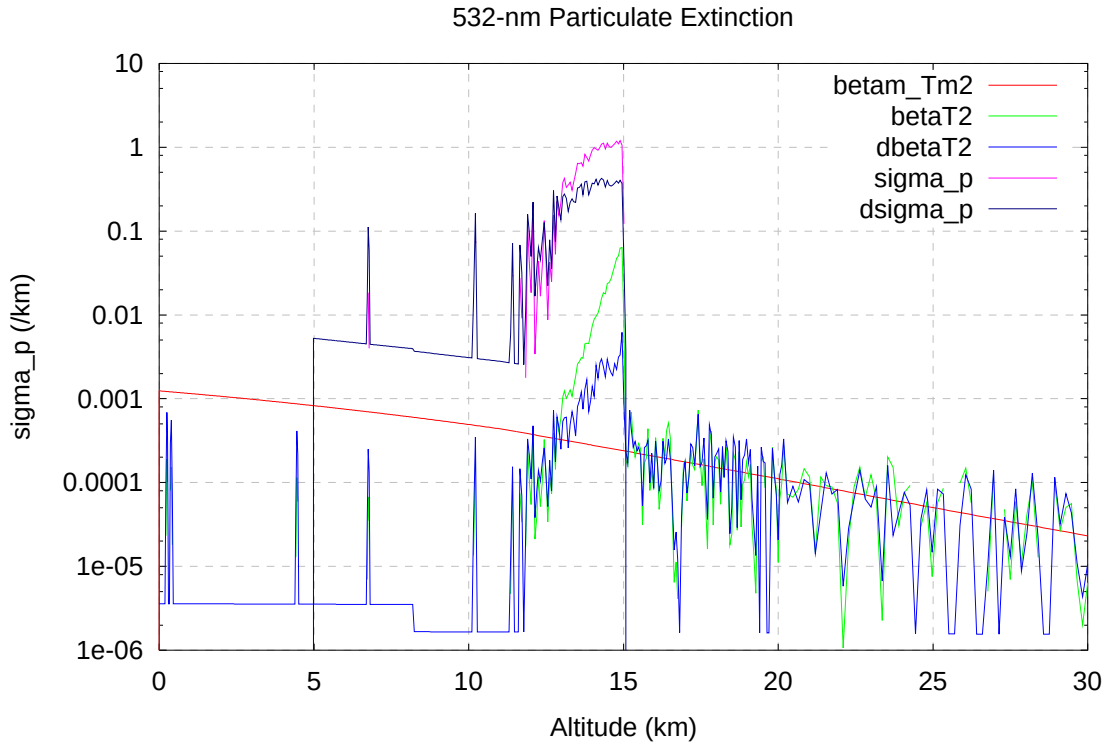

Figure 2: 523-nm simulation 212 representing a cloud with $\tau = 12$. Simulated cloud base is at 5 km. The red line is the attenuated molecular signal; the attenuated backscatter signal (betaT2) is plotted in green with its uncertainty in blue. The retrieved particulate extinction is plotted in magenta with its uncertainty in violet. The lines joining the spikes in the blue and magenta traces are artefacts that result from values smaller than the lower limit of the logarithmic axis.

There are two other side effects that result from the lack of measurable signal from the molecular atmosphere. These are the incorrect normalization of the signal, with a consequent incorrect extinction retrieval, and the incorrect determination of the optical thickness of the feature resulting from a reduced integration interval.

(a) Incorrect normalization of 1064-nm signals

The attenuated backscatter signal at the top of a feature can be written:

$$\beta'(r_t) = (\beta_P(r_t) + \beta_M(r_t))T_M^2(0, r_t)T_P^2(0, r_t - \Delta r)\exp\{-[S_P(r_t)\beta_P(r_t) + S_P(r_t - \Delta r)\beta_P(r_t - \Delta r)]\Delta r\}, \qquad (1)$$

where the subscripts *M* and *P* represent molecular and particulate respectively, β, S and T are the backscatter coefficient, lidar ratio and transmittance, and Δr is the range increment. The top of the feature is defined as that range, r_t, at which the signal first exceeds some threshold, or meets some other criterion. Here it is assumed that a trapezoidal integration is used as in the HERA code. To minimize errors resulting from undetected aerosols, normalization of the 532-nm signal is performed in the supposedly clear air at the point above the feature, $r_t - \Delta r$, and the particulate backscatter retrieved:

$$\beta_P(r_t - \Delta r) = \beta'(r_t - \Delta r)/(T_M^2(0, r_t - \Delta r)T_P^2(0, r_t - \Delta r)) - \beta_M(r_t - \Delta r). \quad (2)$$

Although this is ideally zero, the combination of noise superimposed on the signal, indistinct feature boundaries, and detection thresholds set high enough to avoid false detections triggered by noise, often leads to non-zero values of particulate backscatter. This value is needed to retrieve the backscatter at the cloud top at the next step:

$$\beta_P(r_t) = \beta'(r_t)\exp\{[S_P(r_t)\beta_P(r_t) + S_P(r_t - \Delta r)\beta_P(r_t - \Delta r)]\Delta r\}/(T_M^2(0, r_t)T_P^2(0, r_t - \Delta r)) - \beta_M(r_t). \quad (3)$$

However, at 1064 nm there is usually no measurable signal at r_t - Δr and normalization must be performed at the feature top (the first point in the feature). Following Equation 2:

$$\beta'(r_t)/(T_M^2(0, r_t)T_P^2(0, r_t)) - \beta_M(r_t) = \beta_P(r_t)\exp\{-S_P(r_t)\beta_P(r_t)\Delta r\} - \beta_M(r_t)(1 - \exp\{-S_P(r_t)\beta_P(r_t)\Delta r\}). \quad (4)$$

The quantity that is retrieved is not the true particulate backscatter, but something rather smaller. As this value is used in calculating the transmittance correction at the next range step, the error propagates and grows throughout the feature with the retrieved particulate backscatter being increasingly too small. As the range increment can be 60 m, the calibration error can be six to ten per cent or more in dense clouds. As forward solution algorithms are used in these cases, such large errors can lead to divergent or failed retrievals.

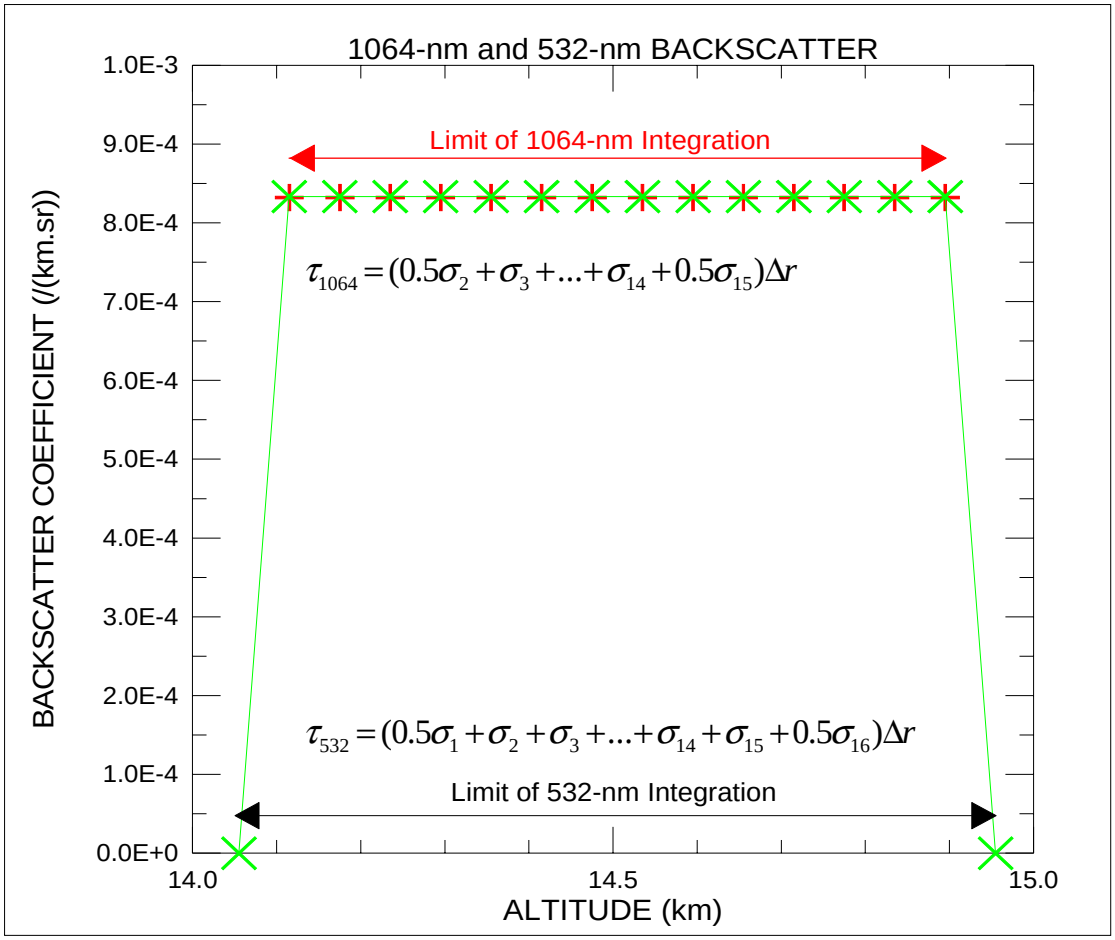

Figure 3: The cause of incorrect optical thickness calculations at 1064 nm. (A trapezoidal integration scheme is used.) The 532-nm signal is plotted using green 'x' with joining lines. The 1064-nm signal is plotted with red '+'. Note the lack of information on the 1064-nm signal beyond the bounds of the feature.

(b) Incorrect optical thickness

As is shown in Figure 3, the lack, at 1064 nm, of measurable signal from the molecular atmosphere leads to incorrect integration of the retrieved extinction when the optical thickness is calculated. As is evidenced by the middle layer in simulation cases 208 and 209, it is not valid simply to assume that the particulate backscatter goes to zero at the adjacent points each end of the feature. Even if the assumption of zero backscatter at the end points could be made, there is no 1064-nm signal to use in the retrieval. The incorrect retrieval of the optical thickness can have further consequences where there are underlying features. As the HERA uses the optical thickness of upper layers to calculate the normalization factor for lower layers, the correction in the case of 1064-nm signals will be inadequate, and the retrieved extinction profile in the next lower feature will be too low. As the retrievals at any altitude are used in calculating the attenuation correction for the next lower altitude, the error in the retrieved profile increases with penetration into the feature. As the range increment can be 60 m, the error can be relatively significant in shallow features. This effect can be seen in the 1064-nm retrieval in the cloud at 10 km in Figure 4. The backscatter at both 532-nm (green trace) and 1064 nm (red trace) in the noise-free simulation are the same, but the retrieved 1064-nm profile is too low at the top of the cloud and gets progressively worse. This problem can also arise in 532-nm retrievals where there are adjacent layers as in test cases 208 and 209.

(c) Proposed corrections

The normalization error in the 1064-nm retrievals results from the lack of knowledge of the backscatter at the altitude immediately before the feature. Two corrections are suggested here. In situations where there is no vertically-adjacent feature detected in the normalization region, the value of particulate backscatter needed in Eq. 1 – 4 to calculate the attenuation over the altitude increment just before the first point in the feature can be obtained from the 532-nm solution, which is performed before the 1064-nm solution. This value would need to be scaled appropriately to correct for the wavelength dependence of the backscatter. As the Scene Classifier Algorithm (SCA) will have already decided on the nature of the feature and its optical properties (lidar ratios) at both wavelengths, the SCA should be able to provide the appropriate scale factor. For situations where there is a vertically-adjacent feature, the value at the base of the previous, overlying feature should be used. At present the information on adjacency is not supplied to the HERA, but a simple upgrade to the current layer flag parameter could inform the HERA whether or not there is an adjacent feature above or below the current feature, or both. This same flag could be used to select the correction to the optical thickness calculation. If there were no adjacent features, then the HERA would use the corresponding, scaled 532-nm values. If there were adjacent features, then the HERA would make the appropriate correction using the values from the adjacent feature.

The result of implementing the suggested changes in the analysis of the simulation shown in Figure 4 is plotted in Figure 5. Integration in the top cloud has been corrected for the “end effects” described above, the normalization correction of the 10-km cloud has used the value from the 532-nm retrieval, and correction for the boundary layer aerosol has used the 532-nm value adjusted for an assumed inverse dependence on wavelength. The 1064-nm retrieval in the clouds now matches the simulated data exactly and is identical to the 532-nm retrieval, which masks it in the plot.

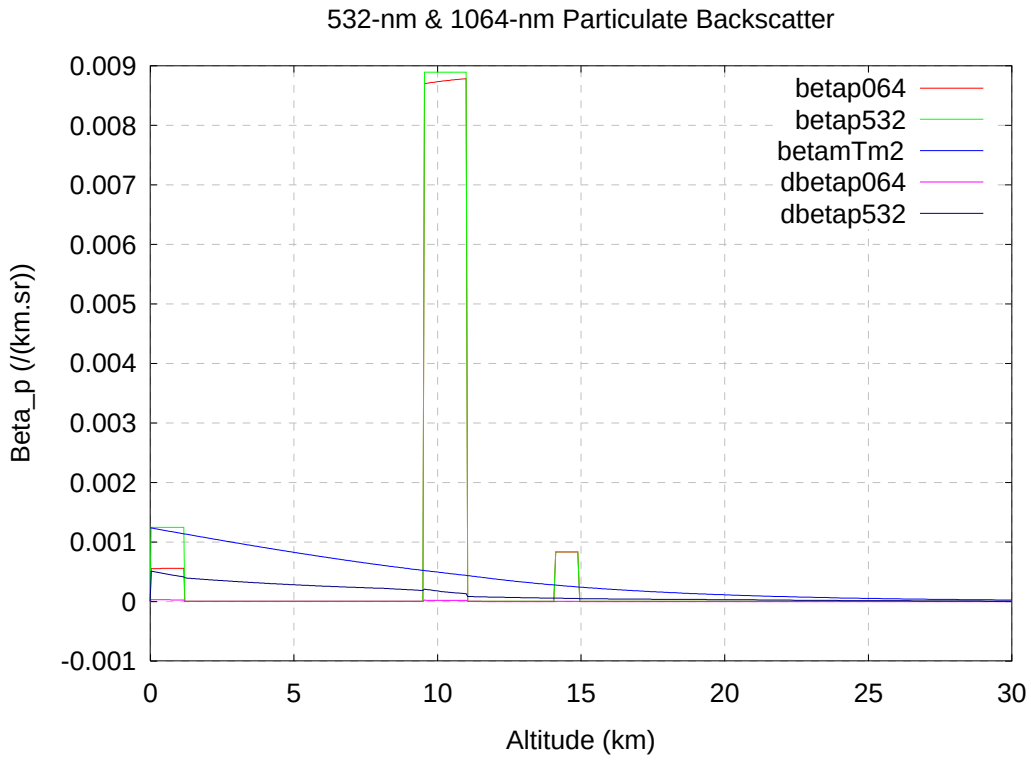

Figure 4: A retrieval using noise-free simulated signals. The retrieved particulate backscatter at 532 nm (green with uncertainty in violet) is exact. The 1064-nm retrieval (red with magenta uncertainty) is correct in the upper feature (the correct normalization factor was supplied) but the optical thickness is incorrect. This error, added to the normalization error described in the text, leads to an underestimate of the particulate backscatter in the lower features, an error that increases with penetration into the cloud. The 1064-nm retrieval in the upper cloud is masked by the 532-nm retrieval, which is identical.

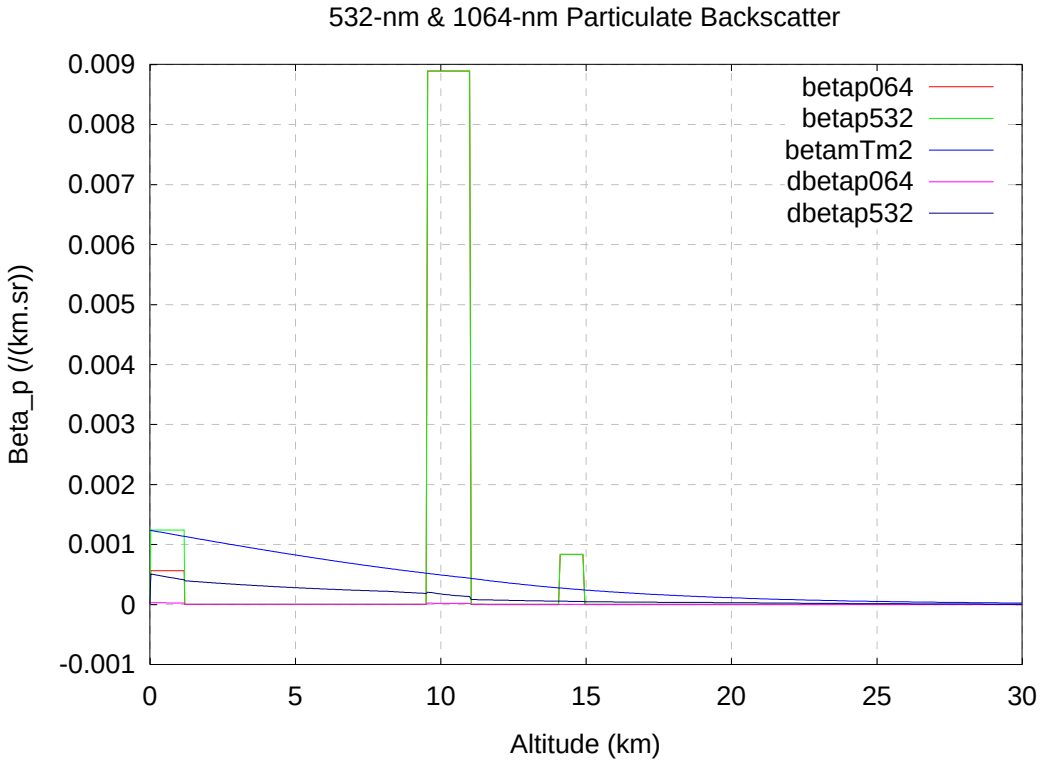

Figure 5: The corrected retrieval of the same simulation as in Figure 4 using the methods described in the text. Note that the 1064-nm retrievals are masked by the 532-nm retrievals, which are identical.

4.5 Limits to the retrieval of parameters and main sources of error.

In this section we examine the test results to see whether there are indications of the range of parameters over which useful retrievals may be obtained. The main factors that are likely to limit the utility of retrievals are weak signals from tenuous targets, high levels of noise (or low SNR), and attenuation of the signal in dense clouds. Another factor, not considered in these tests, is the range ambiguity that results from pulse stretching caused by multiple scattering in dense water clouds. (With its narrow receiver field of view, the CALIPSO lidar is not likely to be susceptible to pulse stretching in cirrus clouds.) Other factors that limit the utility of a retrieval are the uncertainties in the input parameters. An initial qualitative look at some of the main sources of uncertainty and their contributions to the retrieved parameters is made in this section.

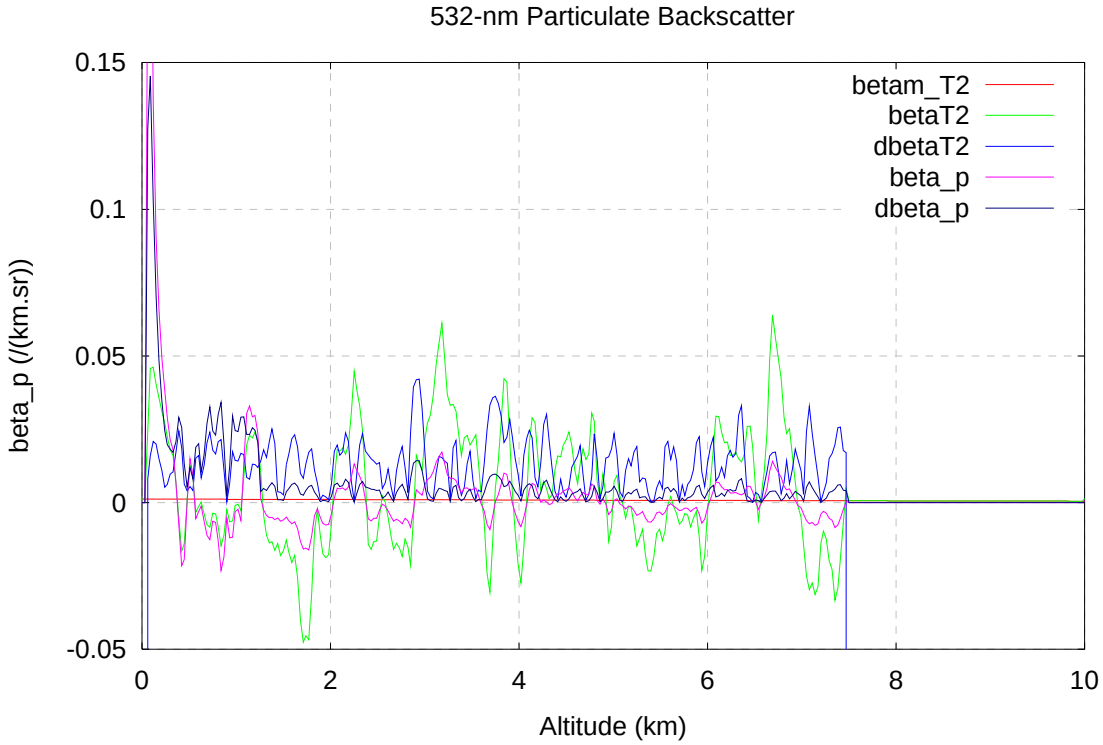

Figure 6: The retrieved 532-nm backscatter (magenta, with uncertainty in violet) for the first 80-km average for Simulation 205. A boundary layer aerosol with a constant backscatter coefficient (β_P = 1.24e-03 $km^{-1}sr^{-1}$) is located between 0.03 and 1.2 km. The rest of the profile contains clear air. The input signal is plotted in green with uncertainty in blue

Consider the results of test cases 204 and 205. These cases contain the same simulated atmospheric scene of a tenuous (τ = 0.02) stratospheric cloud layer around 17 km altitude, a thick cirrus layer (τ = 2.5) around 8 km and a boundary layer aerosol below 1.2 km. The difference between the two cases is that the former simulates nighttime background illumination while the latter simulates daytime conditions. Figures 6 and 7 show the results of the 532-nm analysis of the 80-km horizontal averages for the first two data blocks of simulation 205. The plots are limited to the region below the base of the strong cirrus cloud at 7.5 km. This region supposedly contains a boundary layer aerosol with uniform backscatter coefficient (β_P = 1.24e-03 $km^{-1}sr^{-1}$) below 1.2 km and clear air (β_P = 0) between 1.2 km and cloud base. However no such structure is seen either in the attenuated backscatter input signal (green) or in the retrieved particulate backscatter coefficient. The signal is dominated by noise that has been amplified approximately 150 times after the signal below the strong cirrus has been rescaled to account for the attenuation. The retrieval (magenta) follows the input (green)

in oscillating between positive and negative values that are many times larger than the modelled backscatter. The uncertainty (violet) follows the uncertainty in the input (blue). Figure 7 shows the retrieval for the second 80-km average. Here a successful retrieval could not be obtained with the supplied lidar ratio as the solution diverged near 0.9 km. On the next iteration, the HERA reduced the lidar ratio to prevent the divergence caused by the noisy signal, but the solution then went negative just below this altitude following the noisy input. One can conclude that, in this example of a feature of low backscatter below a dense cloud, there is little useful information in the retrieval. (Note that, in real, operational conditions, it is unlikely that the SIBYL would have detected the boundary layer over the range 0.03 to 1.2 km. In these tests the boundaries were defined using the values supplied to the simulation software.) Figure 8 shows the retrieval for the corresponding region for the nighttime scene. The spikes in the supposedly clear regions near 7.5 km and 10 km result from smoothing of the data during cloud detection and removal in the current version of the SIBYL. As the HERA attempts to set the optical thickness over the clear regions to zero, these spikes cause the retrieved backscatter to go negative in other regions.

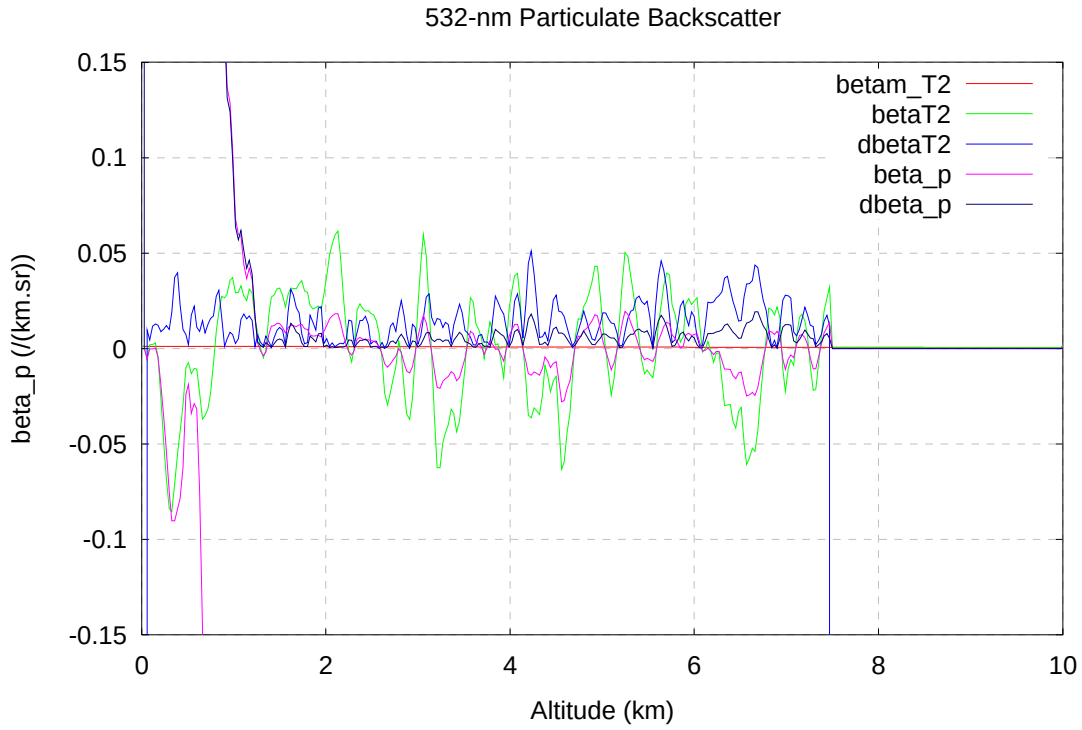

Figure 7: The retrieved backscatter with the correct lidar ratio for the second 80-km average in Simulation 205 showing divergence. The simulated atmosphere, symbols and colours are the same as in Figure 6.

To study the influence of uncertainties in the input parameters on the retrieval, consider the retrieved backscatter coefficients in the thin cloud in simulation 204 plotted in Figure 9. Because the optical thickness is low, the transmittance correction is low and the 33% uncertainty in the lidar ratio contributes little to the uncertainty in the retrieval, which depends primarily on the uncertainty in the attenuated backscatter input signal.

The retrieved particulate extinction coefficient for the same cloud is plotted in Figure 10. It can be seen that the 33% uncertainty in the lidar ratio contributes the major part of the uncertainty in the retrieval. However, because the transmittance corrections are small the uncertainty in the retrieval does not grow noticeably through the depth of the cloud.

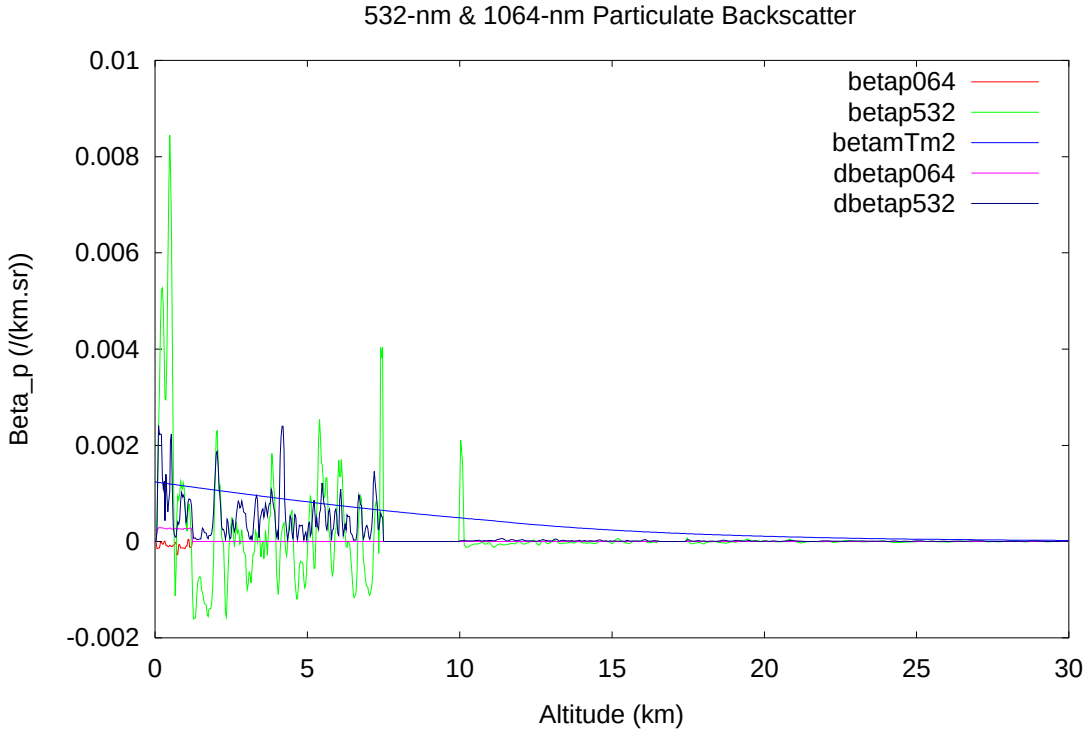

Figure 8: Retrieved backscatter and uncertainties at 532 nm (green and violet) and 1064 nm (red and magenta) for Simulation 204. This is the nighttime version of Simulation 205 shown in Figures 6 and 7. The spikes near 7.5 km and 10km are artefacts of the current cloud detection and removal algorithm.7.5 km and 10km are artefacts of the current cloud detection and removal algorithm artefacts of the current cloud detection and removal algorithm.

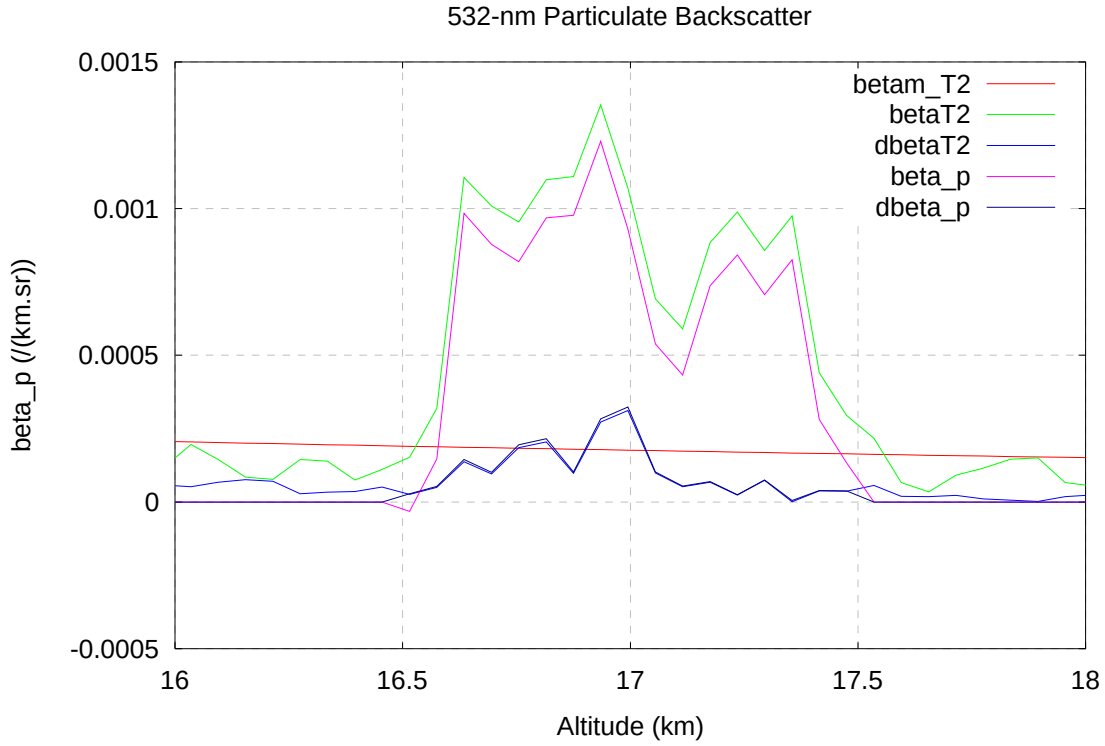

Figure 9: Retrieved 532-nm particulate backscatter for the upper thin cloud of Simulation 204. Colours and symbols are as for Figure 6.

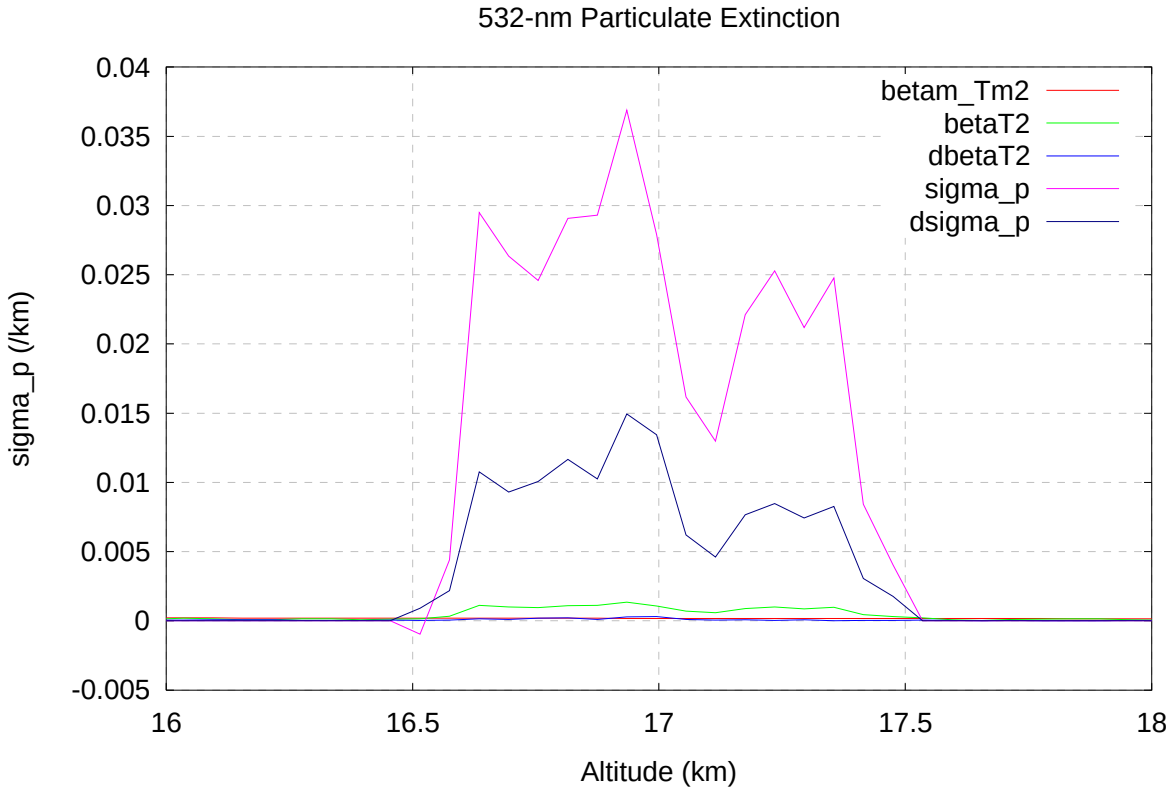

Figure 10: The retrieved particulate extinction coefficient for the same case as in Figure 9. Colours and symbols are as used in Figure 2.

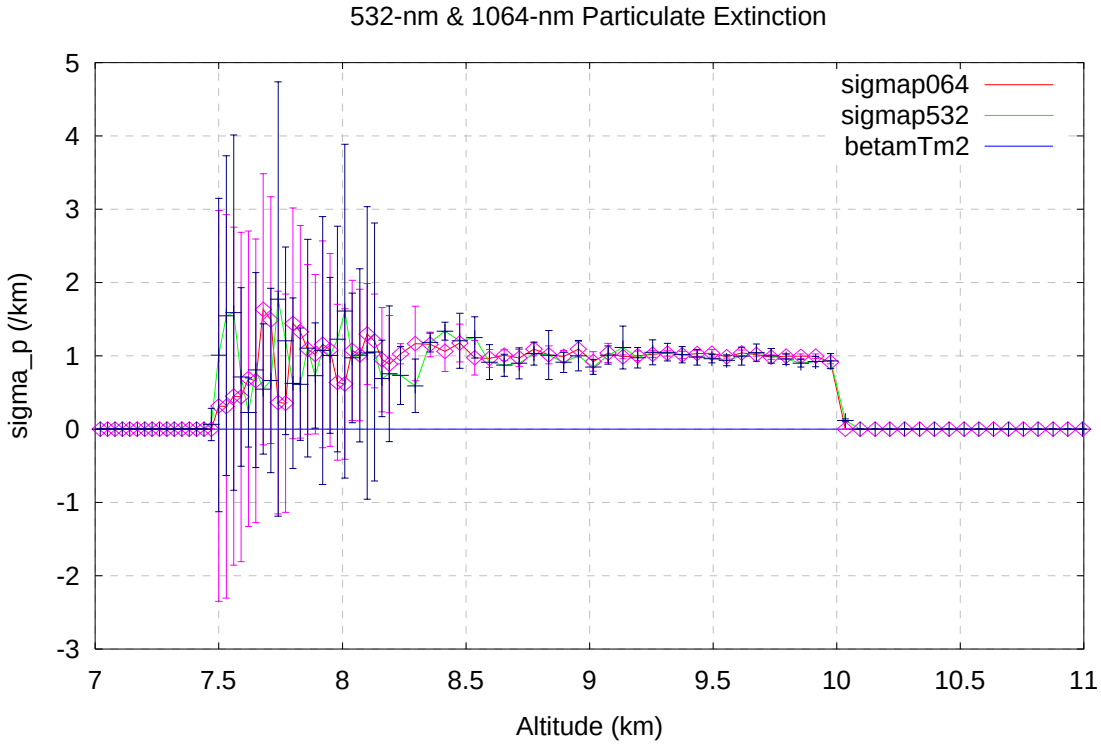

Figure 11: The retrieved extinction coefficients at 532 nm (green with violet symbols and error bars) and 1064 nm (red with magenta symbols and error bars) for the thick cloud (τ = 2.5) in Simulation 204.

Now consider the strong cirrus layer (τ = 2.5) in the same simulations. The HERA was supplied with the correct value of effective transmittance and with values of lidar ratio that varied randomly, from profile to profile, about the true value. As seen in Tables A5 and A6 in Appendix A, and in Figure 11, the HERA was able to retrieve the correct extinction profile and the correct value of optical thickness although, for the reasons explained above, the retrieved lidar ratio was too high. It can also be seen in Figure 11 that the uncertainties grow quite large near the bottom of the cloud. This behaviour contrasts with that seen in the retrieval in the upper cloud where the relative uncertainty is almost constant with range, and is a consequence of the much larger attenuation correction at each range step in the lower cloud.

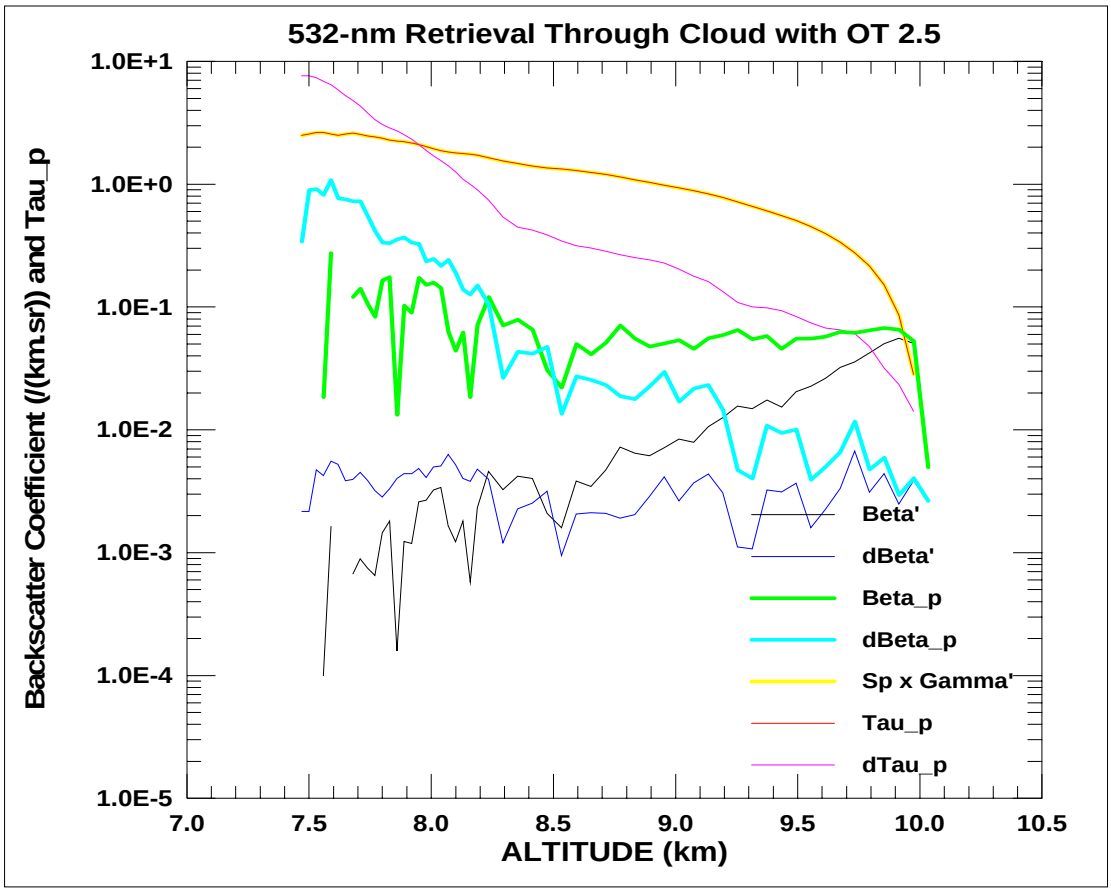

Figure 12: Retrieved 532-nm particulate backscatter coefficient (green with cyan uncertainty) for optically thick (τ = 2.5) cloud in Simulation 205. Retrieved optical thickness profile is plotted in red-yellow with magenta uncertainty. Input signal (attenuated backscatter) is in black with uncertainty in blue.

The growth of the uncertainties in the lower cloud and their main sources can be studied in Figure 12, which shows the backscatter retrieval for the daytime version of the scene where the noise is somewhat larger. Note the step-like increase in uncertainty in the input signal below 8.3 km altitude. This is a result of the change in the vertical resolution and on-board vertical averaging interval from 60 m to 30 m. The change can be seen also in the uncertainties in the retrieved backscatter and optical thickness, which both increase in slope below 8.3 km. Although the fine structure variations in the retrieved backscatter uncertainty reflect those in the uncertainty in the input signal, the steady increase with depth of penetration into the cloud is a consequence of the large attenuation correction and uncertainty in the lidar ratio. (See Young (2002) for a full derivation of the retrieval uncertainties.) It can be seen that the relative uncertainties in both the input signal and the retrieved extinction exceed 100% at 8.5 km altitude and increase to greater than 500-1000% near the base of the

cloud where the signal has been attenuated by a factor of 150. However, because superimposed noise causes points in both the input profile and the retrieved backscatter and extinction profiles go negative, the relative errors in these quantities are not useful parameters for determining at what point to terminate the solution. The uncertainty on the retrieved optical thickness, being an integrated quantity, is far less subject to noise and negative values and could be used to define the point beyond which the uncertainty is too large for the retrieval to be useful.

The noise and widely-varying magnitude of the input signal also affect the rate of convergence of the retrieval. As forward retrievals are used in the case of optically thick clouds, there being little useful signal beneath them that could be used to initiate a more stable backward solution, such retrievals are unstable and highly sensitive to normalization errors, noise and variations in the lidar ratio. An accurate retrieval was possible in this case only because the solution was constrained by a known value of the cloud transmittance. However, at such low levels of SNR, the iterative process of determining the lidar ratio (Young, 2002) is extremely sensitive. Values of lidar ratio that are slightly too high cause the solution to diverge in the positive direction at points where there is a large positive value of noise superimposed on the signal. Conversely, lidar ratios that are slightly too low will cause the solution to diverge in the negative direction, especially where the input is negative. Consequently, the convergence to a final value of the lidar ratio was slow in this test case, and the intermediate solutions varied widely in magnitude. One can conclude that, with SNRs of the magnitude experienced in this example of constrained solution in an optically thick cloud, an optical thickness of about 2.5 is near the limit of what can usefully be analysed.

Finally we consider the example of a tenuous feature and examine the magnitude of the uncertainty in the retrieved backscatter and extinction profiles. The simulation test cases 208 / 209 included three vertically-adjacent aerosol layers, the lowest in contact with the surface. The simulated backscatter levels in all three layers could be considered moderate, and representative of levels typically found in the atmosphere except at very clean locations such as the Southern Ocean. Despite the problems mentioned above, the tests indicate the likely performance of the CALIPSO lidar under fairly typical conditions where surface aerosol layers are unobscured by overlying clouds. Figure 13 shows the profiles of the retrieved backscatter coefficient and uncertainty at both wavelengths in the top two layers. These data for test case 208 (night time) had been averaged to a horizontal resolution of 5 km. At 532 nm it can be seen that the relative uncertainty in both layers is around 100%. At 1064 nm, the uncertainly is a little less, mainly because of the smaller influence of the uncertainty in the molecular profile at 1064 nm in the backscatter retrieval at this longer wavelength. The added uncertainty in the lidar ratio used to convert the backscatter profiles to extinction profiles leads to uncertainties in this latter quantity that are greater than 100%. The 532-nm extinction retrievals are shown in Figure 14. The figure is extended to show the input profile and its uncertainty over the whole altitude range of the signal. The relative uncertainty can be seen to be around 100% over this range. One can conclude that, even in the case of unobscured aerosol layers of moderate strength, measured under nighttime illumination conditions and averaged horizontally over 5 km, the relative uncertainty in the retrieved backscatter and extinction profiles will be greater than about 100%. It may be possible to reduce the uncertainty if additional vertical smoothing were employed. Alternatively, the profiles could be averaged over a larger horizontal distance. The corresponding daytime retrievals in test case 208, which were averaged to 20-km horizontal resolution, showed significantly smaller relative uncertainties.

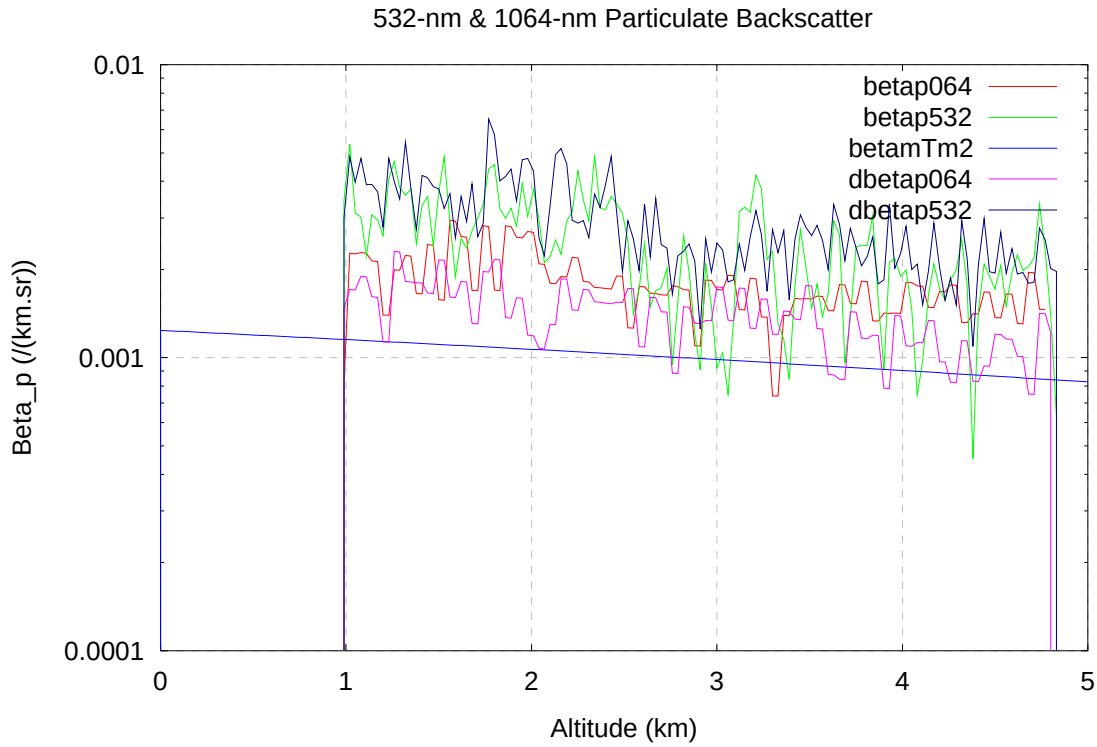

Figure 13: Retrieved backscatter profiles in an aerosol layer of moderate strength, under nighttime illumination and with 5-km horizontal averaging. (Simulation 208) Colours and symbols as in Figure 4.

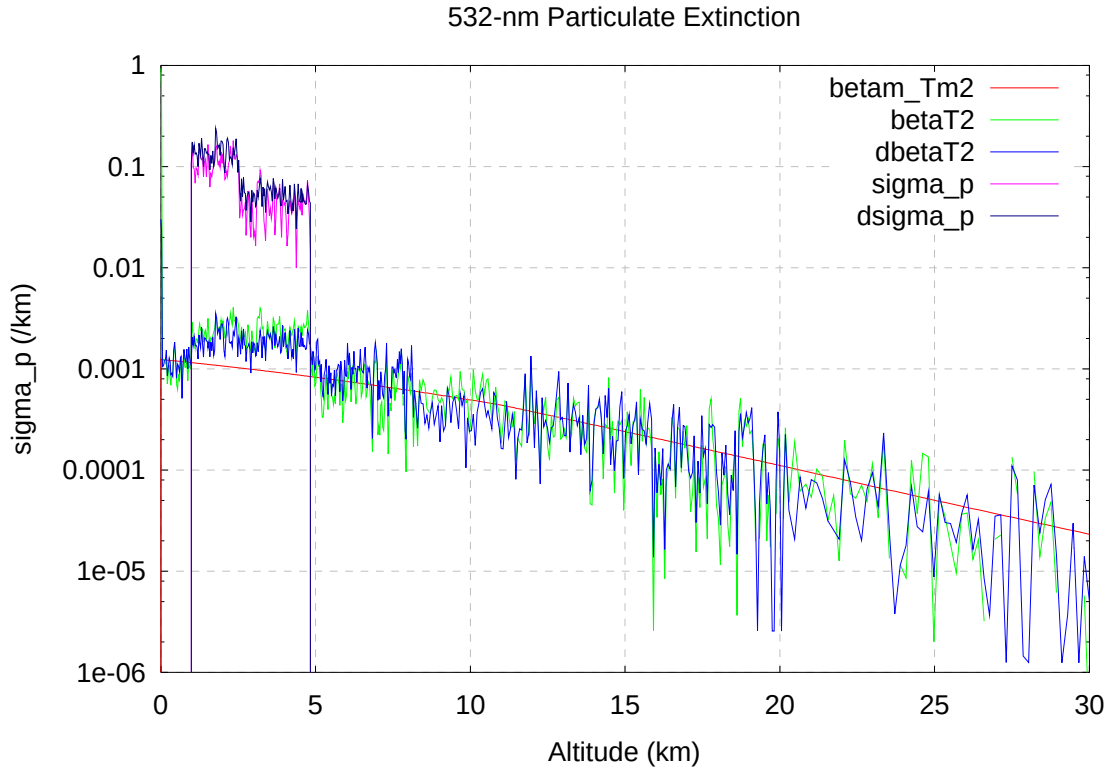

Figure 14: Retrieved 532-nm extinction for the example shown in Figure 13. The uncertainty in the input signal over the complete profile is also shown. Colours and symbols are as in Figure 2.

Conclusions

The Build 2 extinction tests were very successful, not only in testing the accuracy of the performance of the HERA under a variety of simulated signal conditions, but they have also provided initial indications of the limits over which useful parameter retrievals can be obtained.

The accuracy of the HERA was tested using a variety of simulated atmospheric target signals, often combined in one test scene:

1. *Elevated features* ($\tau > 0.1$). HERA was supplied with a correct value of the optical thickness and required to retrieve the correct backscatter and extinction profiles in addition to the lidar ratio. In these cases the solution was constrained using the supplied optical thickness.

2. *Elevated features* ($\tau < 0.1$). The optical thickness was below the detection threshold for SIBYL, so the HERA was supplied with a correct value of the lidar ratio and required to retrieve the correct backscatter and extinction profiles in addition to the particulate optical thickness. These solutions were unconstrained.

3. *Aerosol Layers in contact with the surface or another layer*. The optical thickness was not measurable by the SIBYL, so the HERA was supplied with a correct value of the lidar ratio and required to retrieve the correct backscatter and extinction profiles in addition to the particulate optical thickness. These solutions were unconstrained.

4. *Elevated features with optical thickness high enough to attenuate the lidar signal completely.* These solutions were unconstrained

For the retrievals for the test cases described by the situations in 1 to 3, where the feature was the upper-most feature, or where the SIBYL corrected the signal from the feature for the attenuation of an overlying feature, the HERA retrieved the simulated parameters accurately.

For retrievals where the SIBYL did not correct the signal from a feature for the attenuation caused by an overlying feature, the backscatter retrieved by the HERA was too low by this amount, and the lidar ratio and other parameters were also sometimes affected.

There were two cases (212 and 213) where optical thickness was large enough to attenuate the simulated signal completely. Because the input signal did not reproduce the whole depth of the profile, it was not possible for the retrieval algorithm to retrieve the optical thickness. Also, at such high optical thickness, the forward solutions that are necessarily employed are extremely sensitive to errors in signal calibration and zero level, the lidar ratio employed and, to a lesser extent, the numerical precision of the calculations. As such retrievals are unconstrained, the performance of any retrieval algorithm will be highly variable. It is probably not realistic to attempt unconstrained solution profiles over penetration depths with optical thicknesses greater than about unity, although this requires further examination.

The tests also provided insight as to the limits over which useful values of the optical parameters of various atmospheric targets could be obtained.

1. For constrained solutions under the SNR levels used in the tests, useful retrievals are limited to features with an optical thickness less than about 2.5.
2. For aerosol layers of backscatter strengths typically found in the atmosphere, the relative uncertainty in the retrieved profiles will be greater than or of the order of 100%, unless additional vertical smoothing is used or the profiles are averaged over more than 5-km horizontal distance.
3. For tenuous features underlying optically thick features ($\tau > 2.5$), no useful retrieval can be obtained. Additional vertical averaging is unlikely to help in these cases.
4. For optically-thick features in which the signal is totally attenuated, solutions are unconstrained and useful retrievals are limited, probably to penetration depths with optical thicknesses less than about unity.

Finally, some recommendations are made regarding actions required to further the development and testing of the extinction retrieval algorithms.

1. The signals from features need to be corrected for the attenuation of overlying features detected at different horizontal averaging resolutions, either in the SIBYL module before passing to the HERA, or in the HERA. Where the SIBYL is unable to determine the magnitude of this attenuation, the correction should be done in the HERA module.
2. Consideration should be given to the correction of 1064-nm normalization and optical thickness calculations using information from the 532-nm retrieval, scaled appropriately for wavelength, for the same signal region.
3. The parameters passed by the SCA need to inform the HERA whether a feature has other features, detected at other horizontal averaging resolutions, in contact with either the top or base of the feature, or both. This would enable the solution to the current problem of vertically adjacent or embedded features. A table summarizing the data for all detected features in all profiles in an 80-km data block should appear at the start of the data block.
4. The most appropriate parameters for determining when a solution should be terminated need to be defined. It is suggested that the relative uncertainty in the retrieved optical thickness is a good candidate, as it is less subject to the noise variations experienced in the backscatter and extinction profile data.
5. Further test cases are required to enable a tighter specification of the likely limits of useful retrievals in various situations.
6. The degree to which additional vertical smoothing of data can be used to improve the SNR of tenuous features, yet still be consistent with requirements for the vertical resolution of the output profiles, should be examined.
7. The interpretation in both the HERA and SIBYL modules of the mutual data interface should be checked in detail.
8. The input files used for the test cases should be checked and corrected.

   (a) The boundary indices defined for the features should be checked against the profile data to remove cases of signal leakage into the supposedly clear regions. (The next version of the SIBYL will correct this problem.)

   (b) Feature boundary indices, defined as the first range index in a feature at which the signal exceeds some threshold, should be checked to ensure that there is valid signal at those range indices, and that the signal uncertainties are defined.

Acknowledgments

The author gratefully acknowledges the collaboration of Mark Vaughan in the development of the SIBYL-HERA-EOPT interface and analysis framework, and in the definition, setting up and running of the test cases in the Build 2 tests.

Figures 1 is reproduced from Vaughan et al. (2002) and the Tables 1 and 2 have similarly been taken (with modification) from that work. The summary tables in Appendix A were produced by Mark Vaughan using the results of the HERA Build 2 performance tests run by Jim Lambeth of SAIC.

The simulated data files used in the Build 2 tests were produced by Kathy Powell of SAIC.

This work is supported by NASA Langley Research Center under contracts NAS1-19570 and NAS1-02058.

References

Anselmo, T., R. Bergman, R. Clifton, J. Lambeth, K.-P. Lee and S. Rodier (2002). Cloud-Aerosol LIDAR Infrared Pathfinder Satellite Observations Data Management System, LIDAR Subsystem, Build 2 Test Summary Report, Document PC-SCI-304, Science Applications International Corporation, 124 pp.

Vaughan, M., S. Young, J. Lambeth, R. Bergman, T. Murray (2002). Build 2 Extinction Testing and Test Results. Paper presented at the sixth CALIPSO Science Team Meeting, Hampton Va., May 23- 25, 2002.

Vaughan, M. A., D. M. Winker and C. A. Hostetler (2002). SIBYL: a selective iterated boundary location algorithm for finding cloud and aerosol layers in CALIPSO data, In: Lidar Remote Sensing in Atmospheric and Earth Sciences: reviewed and revised papers presented at the twenty-first International Laser Radar Conference (ILRC21), Québec, Canada, L. R. Bissonnette, G. Roy and G. Vallée (editors) Québec, Defence R&D Canada, Valcartier, pp 791- 794.

Winker, D. M., J. Pelon and M. P. McCormick (2002). The CALIPSO Mission: Aerosol and Cloud Observations from Space, In: Lidar Remote Sensing in Atmospheric and Earth Sciences: reviewed and revised papers presented at the twenty-first International Laser Radar Conference (ILRC21), Québec, Canada, L. R. Bissonnette, G. Roy and G. Vallée (editors) Québec, Defence R&D Canada, Valcartier, pp 735- 738.

Young, S. A. (1995). Lidar analysis of lidar backscatter profiles in optically thin clouds. *Applied Optics,* **34,** 7019-7031.

Young, S. A., (2001a). Notes on the Use of the eOPT / HERA Software. Report to NASA Langley Research Center, Dec. 13th 2001, prepared under SAIC Contract NAS1-19570. CSIRO Atmospheric Research Internal Paper No. 23, 12 pp.

Young, S. A., (2001b). Results of testing the eOPT / HERA software on simulated data. Report to NASA Langley Research Center, Dec. 13th 2001, prepared under SAIC Contract NAS1-19570. CSIRO Atmospheric Research Internal Paper No. 24, 14 pp.

Young, S. A. (2002). The Hybrid Extinction Retrieval Algorithms (HERA) for the analysis of lidar data from space. Report to NASA Langley Research Center, February 2002, prepared under SAIC Contracts NAS1-19570 and NAS1-02058, CSIRO Atmospheric Research Technical Paper 54, 28 pp.

Young, S. A., M. A. Vaughan and D. M. Winker (2002). Adaptive methods for retrieving extinction profiles from space applied to CALIPSO lidar data. In: Lidar Remote Sensing in Atmospheric and Earth Sciences: reviewed and revised papers presented at the twenty-first International Laser Radar Conference (ILRC21), Québec, Canada, L .R. Bissonnette, G. Roy and G. Vallée (editors) Québec, Defence R&D Canada, Valcartier, pp 743- 746.

APPENDIX A: Summary of the Results of the Build 2 tests.

Table A1. Simulation Case 200A.

TEST 200A

Grid= 5.00000 Km

Feature # 1 Top= 12.015 Km Base= 9.975 Km

Parameter	Min	Max	Mean	StDev	Target
532 Lidar Ratio	23.7148	26.3684	25.0989	0.6084	25.0000
064 Lidar Ratio	25.0000	25.0000	25.0000	0.0000	25.0000
532 Optical Depth	0.5000	0.5000	0.5000	0.0000	0.5000
064 Optical Depth	0.4691	0.5152	0.4900	0.0096	0.5000
532 Ext Coeff	0.0317	0.3762	0.2381	0.0524	0.2500
064 Ext Coeff	0.0287	0.3136	0.2353	0.0438	0.2500
532 Backscatter	1.22e-03	1.53e-02	9.49e-03	2.10e-03	1.00e-02
064 Backscatter	1.15e-03	1.25e-02	9.41e-03	1.75e-03	1.00e-02
532 Color Ratio	0.9343	1.0914	1.0120	0.0349	1.0000
532 Vert Ext SD	0.0460	0.0624			
064 Vert Ext SD	0.0391	0.0497			
532 Horz Ext SD	0.0114	0.0431			
064 Horz Ext SD	0.0078	0.0214			

Grid= 20.0000 Km

Feature # 1 Top= 2.490 Km Base= 0.030 Km

Parameter	Min	Max	Mean	StDev	Target
532 Lidar Ratio	60.9000	60.9000	60.9000	0.0000	60.9000
064 Lidar Ratio	45.9000	45.9000	45.9000	0.0000	45.9000
532 Optical Depth	0.1532	0.2261	0.1882	0.0228	0.2000
064 Optical Depth	0.0072	0.0271	0.0154	0.0041	0.0600
532 Ext Coeff	-0.0292	0.2088	0.0759	0.0360	0.0800
064 Ext Coeff	-0.0149	0.0252	0.0062	0.0069	0.0240
532 Backscatter	-4.80e-04	3.43e-03	1.25e-03	5.90e-04	1.31e-03
064 Backscatter	-3.25e-04	5.49e-04	1.36e-04	1.50e-04	5.23e-04
532 Color Ratio	0.1106	0.7367	0.2443	0.1334	0.3968
532 Vert Ext SD	0.0305	0.0414			
064 Vert Ext SD	0.0058	0.0080			
532 Horz Ext SD	0.0000	0.0516			
064 Horz Ext SD	0.0000	0.0089			

Grid= 80.0000 Km

No Features Detected

Table A2. Simulation Case 201A.

TEST 201A

Grid= 5.00000 Km

Feature # 1 Top= 12.015 Km Base= 9.975 Km

Parameter	Min	Max	Mean	StDev	Target
532 Lidar Ratio	22.9125	29.1912	25.1345	0.9993	25.0000
064 Lidar Ratio	25.0000	25.0000	25.0000	0.0000	25.0000
532 Optical Depth	0.5000	0.5000	0.5000	0.0000	0.5000
064 Optical Depth	0.4479	0.5191	0.4886	0.0147	0.5000
532 Ext Coeff	-0.0764	0.4521	0.2380	0.0643	0.2500
064 Ext Coeff	0.0093	0.3413	0.2346	0.0464	0.2500
532 Backscatter	-3.03e-03	1.86e-02	9.48e-03	2.58e-03	1.00e-02
064 Backscatter	3.71e-04	1.37e-02	9.38e-03	1.86e-03	1.00e-02
532 Color Ratio	0.9150	1.6215	1.0557	0.1014	1.0000
532 Vert Ext SD	0.0487	0.0837			
064 Vert Ext SD	0.0333	0.0563			
532 Horz Ext SD	0.0254	0.0694			
064 Horz Ext SD	0.0110	0.0355			

Grid= 20.0000 Km

No Features Detected

Grid= 80.0000 Km

Feature # 1 Top= 2.490 Km Base= 0.030 Km

Parameter	Min	Max	Mean	StDev	Target
532 Lidar Ratio	60.9000	60.9000	60.9000	0.0000	60.9000
064 Lidar Ratio	45.9000	45.9000	45.9000	0.0000	45.9000
532 Optical Depth	0.1192	0.2669	0.2186	0.0540	0.2000
064 Optical Depth	0.0140	0.0187	0.0158	0.0017	0.0600
532 Ext Coeff	-0.7276	0.3472	0.0873	0.0575	0.0800
064 Ext Coeff	-0.0104	0.0223	0.0064	0.0052	0.0240
532 Backscatter	-1.19e-02	5.70e-03	1.43e-03	9.43e-04	1.31e-03
064 Backscatter	-2.27e-04	4.86e-04	1.40e-04	1.14e-04	5.23e-04
532 Color Ratio	0.0914	0.2996	0.1541	0.0734	0.3968
532 Vert Ext SD	0.0309	0.1028			
064 Vert Ext SD	0.0048	0.0059			
532 Horz Ext SD	0.0000	0.3549			
064 Horz Ext SD	0.0000	0.0088			

Table A3. Simulation Case 202A.

TEST 202A

Grid= 5.00000 Km

Feature # 1 Top= 10.995 Km Base= 9.495 Km

Parameter	Min	Max	Mean	StDev	Target
532 Lidar Ratio	21.2397	25.5376	23.4503	0.7733	22.5000
064 Lidar Ratio	22.5000	22.5000	22.5000	0.0000	22.5000
532 Optical Depth	0.3000	0.3000	0.3000	0.0000	0.3000
064 Optical Depth	0.2635	0.2873	0.2761	0.0049	0.3000
532 Ext Coeff	0.0632	0.3170	0.1922	0.0330	0.2000
064 Ext Coeff	0.0757	0.2252	0.1814	0.0227	0.2000
532 Backscatter	2.56e-03	1.35e-02	8.21e-03	1.44e-03	8.89e-03
064 Backscatter	3.36e-03	1.00e-02	8.06e-03	1.01e-03	8.89e-03
532 Color Ratio	0.8849	1.1002	1.0014	0.0400	1.0000
532 Vert Ext SD	0.0234	0.0455			
064 Vert Ext SD	0.0187	0.0291			
532 Horz Ext SD	0.0157	0.0319			
064 Horz Ext SD	0.0072	0.0137			

Grid= 20.0000 Km

Feature # 1 Top= 1.200 Km Base= 0.030 Km

Parameter	Min	Max	Mean	StDev	Target
532 Lidar Ratio	40.2890	40.2890	40.2890	0.0000	40.2890
064 Lidar Ratio	27.2590	27.2590	27.2590	0.0000	27.2590
532 Optical Depth	0.0453	0.0672	0.0527	0.0060	0.0600
064 Optical Depth	0.0055	0.0113	0.0080	0.0015	0.0183
532 Ext Coeff	-0.0105	0.1042	0.0444	0.0200	0.0500
064 Ext Coeff	-0.0077	0.0203	0.0068	0.0046	0.0152
532 Backscatter	-2.60e-04	2.59e-03	1.10e-03	4.98e-04	1.24e-03
064 Backscatter	-2.83e-04	7.46e-04	2.49e-04	1.68e-04	5.58e-04
532 Color Ratio	0.1891	0.6704	0.3189	0.1065	0.4500
532 Vert Ext SD	0.0152	0.0251			
064 Vert Ext SD	0.0032	0.0059			
532 Horz Ext SD	0.0000	0.0262			
064 Horz Ext SD	0.0000	0.0049			

(Continued on next page)

Feature # 2 Top= 17.415 Km   Base= 16.575 Km

Parameter	Min	Max	Mean	StDev	Target
532 Lidar Ratio	30.0000	30.0000	30.0000	0.0000	30.0000
064 Lidar Ratio	30.0000	30.0000	30.0000	0.0000	30.0000
532 Optical Depth	0.0178	0.0227	0.0201	0.0015	0.0200
064 Optical Depth	0.0179	0.0208	0.0194	0.0009	0.0200
532 Ext Coeff	-0.0008	0.0386	0.0226	0.0076	0.0250
064 Ext Coeff	-0.0049	0.0376	0.0220	0.0073	0.0250
532 Backscatter	-2.74e-05	1.29e-03	7.54e-04	2.52e-04	8.33e-04
064 Backscatter	-1.64e-04	1.25e-03	7.34e-04	2.43e-04	8.33e-04
532 Color Ratio	0.8720	1.3049	1.0473	0.1300	1.0000
532 Vert Ext SD	0.0061	0.0089			
064 Vert Ext SD	0.0048	0.0093			
532 Horz Ext SD	0.0026	0.0057			
064 Horz Ext SD	0.0032	0.0055			

Grid=   80.0000 Km

No Features Detected

Table A4. Simulation Case 203A.

TEST 203A

Grid= 5.00000 Km

Feature # 1 Top= 10.995 Km Base= 9.495 Km

Parameter	Min	Max	Mean	StDev	Target
532 Lidar Ratio	20.5516	27.6725	23.4128	1.1387	22.5000
064 Lidar Ratio	22.5000	22.5000	22.5000	0.0000	22.5000
532 Optical Depth	0.3000	0.3000	0.3000	0.0000	0.3000
064 Optical Depth	0.2586	0.2956	0.2747	0.0072	0.3000
532 Ext Coeff	0.0288	0.3194	0.1922	0.0411	0.2000
064 Ext Coeff	0.0607	0.2385	0.1805	0.0250	0.2000
532 Backscatter	1.24e-03	1.48e-02	8.23e-03	1.80e-03	8.89e-03
064 Backscatter	2.70e-03	1.06e-02	8.02e-03	1.11e-03	8.89e-03
532 Color Ratio	0.8888	1.2173	1.0157	0.0636	1.0000
532 Vert Ext SD	0.0300	0.0562			
064 Vert Ext SD	0.0204	0.0304			
532 Horz Ext SD	0.0254	0.0467			
064 Horz Ext SD	0.0103	0.0198			

Grid= 20.0000 Km

No Features Detected

Grid= 80.0000 Km

Feature # 1 Top= 1.200 Km Base= 0.030 Km

Parameter	Min	Max	Mean	StDev	Target
532 Lidar Ratio	40.2890	40.2890	40.2890	0.0000	40.2890
064 Lidar Ratio	27.2590	27.2590	27.2590	0.0000	27.2590
532 Optical Depth	0.0410	0.0633	0.0565	0.0080	0.0600
064 Optical Depth	0.0066	0.0086	0.0079	0.0007	0.0183
532 Ext Coeff	-0.1094	0.1753	0.0474	0.0221	0.0500
064 Ext Coeff	-0.0041	0.0156	0.0067	0.0033	0.0152
532 Backscatter	-2.72e-03	4.35e-03	1.18e-03	5.49e-04	1.24e-03
064 Backscatter	-1.52e-04	5.73e-04	2.45e-04	1.20e-04	5.58e-04
532 Color Ratio	0.1985	0.3022	0.2478	0.0382	0.4500
532 Vert Ext SD	0.0122	0.0305			
064 Vert Ext SD	0.0026	0.0039			
532 Horz Ext SD	0.0000	0.1050			
064 Horz Ext SD	0.0000	0.0043			

Feature # 2 Top= 17.415 Km Base= 16.575 Km

(Continued on next page)

Parameter	Min	Max	Mean	StDev	Target
532 Lidar Ratio	30.0000	30.0000	30.0000	0.0000	30.0000
064 Lidar Ratio	30.0000	30.0000	30.0000	0.0000	30.0000
532 Optical Depth	0.0172	0.0208	0.0189	0.0013	0.0200
064 Optical Depth	0.0178	0.0212	0.0194	0.0014	0.0200
532 Ext Coeff	0.0019	0.0327	0.0213	0.0071	0.0250
064 Ext Coeff	-0.0003	0.0337	0.0220	0.0072	0.0250
532 Backscatter	6.40e-05	1.09e-03	7.11e-04	2.38e-04	8.33e-04
064 Backscatter	-1.08e-05	1.12e-03	7.33e-04	2.41e-04	8.33e-04
532 Color Ratio	0.9671	1.3405	1.1042	0.1498	1.0000
532 Vert Ext SD	0.0047	0.0080			
064 Vert Ext SD	0.0065	0.0088			
532 Horz Ext SD	0.0027	0.0064			
064 Horz Ext SD	0.0012	0.0061			

Table A5. Simulation Case 204A.

TEST 204A

Grid= 5.00000 Km

Feature # 1 Top= 9.975 Km Base= 7.500 Km

Parameter	Min	Max	Mean	StDev	Target
532 Lidar Ratio	15.5920	16.9494	16.2080	0.2840	15.0000
064 Lidar Ratio	14.8500	15.0000	14.9953	0.0262	15.0000
532 Optical Depth	2.0330	2.7516	2.4909	0.0743	2.5000
064 Optical Depth	0.9357	1.0718	1.0056	0.0235	2.5000
532 Ext Coeff	-0.0213	2.9504	0.9810	0.2804	1.0000
064 Ext Coeff	-0.0540	0.8858	0.3386	0.2766	1.0000
532 Backscatter	-1.31e-03	1.84e-01	6.05e-02	1.73e-02	6.67e-02
064 Backscatter	-3.60e-03	5.91e-02	2.26e-02	1.84e-02	6.67e-02
532 Color Ratio	0.3437	0.4527	0.3880	0.0206	1.0000
532 Vert Ext SD	0.1713	0.4906			
064 Vert Ext SD	0.2672	0.2947			
532 Horz Ext SD	0.0397	0.5189			
064 Horz Ext SD	0.0104	0.0351			

Grid= 20.0000 Km

Feature # 1 Top= 17.415 Km Base= 16.575 Km

Parameter	Min	Max	Mean	StDev	Target
532 Lidar Ratio	30.0000	30.0000	30.0000	0.0000	30.0000
064 Lidar Ratio	30.0000	30.0000	30.0000	0.0000	30.0000
532 Optical Depth	0.0174	0.0216	0.0198	0.0011	0.0200
064 Optical Depth	0.0182	0.0217	0.0200	0.0010	0.0200
532 Ext Coeff	-0.0002	0.0378	0.0222	0.0077	0.0250
064 Ext Coeff	-0.0023	0.0349	0.0226	0.0078	0.0250
532 Backscatter	-6.45e-06	1.26e-03	7.41e-04	2.56e-04	8.33e-04
064 Backscatter	-7.78e-05	1.16e-03	7.52e-04	2.61e-04	8.33e-04
532 Color Ratio	0.8543	1.2700	1.0610	0.1160	1.0000
532 Vert Ext SD	0.0059	0.0096			
064 Vert Ext SD	0.0067	0.0103			
532 Horz Ext SD	0.0033	0.0061			
064 Horz Ext SD	0.0025	0.0055			

(Continued on next page)

Grid= 80.0000 Km

Feature # 1 Top= 1.200 Km Base= 0.030 Km

Parameter	Min	Max	Mean	StDev	Target
532 Lidar Ratio	40.2890	40.2890	40.2890	0.0000	40.2890
064 Lidar Ratio	27.2590	27.2590	27.2590	0.0000	27.2590
532 Optical Depth	-0.0128	0.1123	0.0558	0.0439	0.0600
064 Optical Depth	-0.0034	-0.0021	-0.0027	0.0005	0.0183
532 Ext Coeff	-0.0652	0.3400	0.0465	0.0727	0.0500
064 Ext Coeff	-0.0073	0.0011	-0.0023	0.0019	0.0152
532 Backscatter	-1.62e-03	8.44e-03	1.15e-03	1.81e-03	1.24e-03
064 Backscatter	-2.68e-04	3.92e-05	-8.41e-05	6.89e-05	5.58e-04
532 Color Ratio	0.0000	0.1008	0.0268	0.0381	0.4500
532 Vert Ext SD	0.0245	0.1003			
064 Vert Ext SD	0.0015	0.0023			
532 Horz Ext SD	0.0000	0.1354			
064 Horz Ext SD	0.0000	0.0027			

Table A6. Simulation Case 205A.

TEST 205A

Grid= 5.00000 Km

Feature # 1 Top= 9.975 Km Base= 7.500 Km

Parameter	Min	Max	Mean	StDev	Target
532 Lidar Ratio	15.1145	17.2543	16.1772	0.3759	15.0000
064 Lidar Ratio	15.0000	15.0000	15.0000	0.0000	15.0000
532 Optical Depth	-0.2842	2.6995	2.4231	0.3118	2.5000
064 Optical Depth	0.9574	1.0833	1.0107	0.0271	2.5000
532 Ext Coeff	-150.6081	24.9695	0.9400	2.5269	1.0000
064 Ext Coeff	-0.1361	0.8968	0.3402	0.2804	1.0000
532 Backscatter	-9.50e+00	1.57e+00	5.82e-02	1.58e-01	6.67e-02
064 Backscatter	-9.07e-03	5.98e-02	2.27e-02	1.87e-02	6.67e-02
532 Color Ratio	0.3817	1.0614	0.5024	0.1112	1.0000
532 Vert Ext SD	0.5618	21.2657			
064 Vert Ext SD	0.2556	0.2979			
532 Horz Ext SD	0.0496	15.6971			
064 Horz Ext SD	0.0123	0.0654			

Grid= 20.0000 Km

Feature # 1 Top= 17.415 Km Base= 16.575 Km

Parameter	Min	Max	Mean	StDev	Target
532 Lidar Ratio	30.0000	30.0000	30.0000	0.0000	30.0000
064 Lidar Ratio	30.0000	30.0000	30.0000	0.0000	30.0000
532 Optical Depth	0.0099	0.0333	0.0207	0.0056	0.0200
064 Optical Depth	0.0157	0.0233	0.0199	0.0019	0.0200
532 Ext Coeff	-0.0250	0.0704	0.0234	0.0164	0.0250
064 Ext Coeff	-0.0094	0.0465	0.0226	0.0095	0.0250
532 Backscatter	-8.32e-04	2.35e-03	7.79e-04	5.46e-04	8.33e-04
064 Backscatter	-3.12e-04	1.55e-03	7.53e-04	3.15e-04	8.33e-04
532 Color Ratio	0.7266	13.0787	2.0572	2.4666	1.0000
532 Vert Ext SD	0.0100	0.0222			
064 Vert Ext SD	0.0058	0.0120			
532 Horz Ext SD	0.0112	0.0191			
064 Horz Ext SD	0.0059	0.0091			

(Continued on next page)

Grid= 80.0000 Km

Feature # 1 Top= 1.200 Km Base= 0.030 Km

Parameter	Min	Max	Mean	StDev	Target
532 Lidar Ratio	14.7471	40.2890	33.0070	10.2231	40.2890
064 Lidar Ratio	27.2590	27.2590	27.2590	0.0000	27.2590
532 Optical Depth	-0.5665	1.9253	0.3891	0.9126	0.0600
064 Optical Depth	-0.0045	-0.0028	-0.0033	0.0007	0.0183
532 Ext Coeff	-17.5402	18.0584	0.3192	3.8879	0.0500
064 Ext Coeff	-0.0108	0.0040	-0.0029	0.0035	0.0152
532 Backscatter	-1.01e+00	1.06e+00	1.94e-02	1.69e-01	1.24e-03
064 Backscatter	-3.98e-04	1.48e-04	-1.05e-04	1.27e-04	5.58e-04
532 Color Ratio	0.0000	0.0600	0.0130	0.0236	0.4500
532 Vert Ext SD	0.4200	6.3356			
064 Vert Ext SD	0.0026	0.0042			
532 Horz Ext SD	0.0000	7.4453			
064 Horz Ext SD	0.0000	0.0048			

Table A7. Simulation Case 206A.

TEST 206A

Grid= 5.00000 Km

Feature # 1 Top= 4.800 Km Base= 0.990 Km

Parameter	Min	Max	Mean	StDev	Target
532 Lidar Ratio	20.0541	24.0697	22.0467	1.0198	21.9790
064 Lidar Ratio	31.3720	31.3720	31.3720	0.0000	31.3720
532 Optical Depth	0.1710	0.1710	0.1710	0.0000	0.1710
064 Optical Depth	0.1716	0.2149	0.1938	0.0090	0.1960
532 Ext Coeff	-0.0102	0.1169	0.0445	0.0172	0.0450
064 Ext Coeff	-0.0150	0.0991	0.0506	0.0126	0.0515
532 Backscatter	-4.75e-04	5.39e-03	2.02e-03	7.85e-04	2.05e-03
064 Backscatter	-4.78e-04	3.16e-03	1.61e-03	4.03e-04	1.64e-03
532 Color Ratio	0.8210	12.3665	1.1239	1.1710	0.8020
532 Vert Ext SD	0.0143	0.0211			
064 Vert Ext SD	0.0087	0.0151			
532 Horz Ext SD	0.0108	0.0207			
064 Horz Ext SD	0.0089	0.0153			

Grid= 20.0000 Km

No Features Detected

Grid= 80.0000 Km

No Features Detected

Table A8. Simulation Case 207A.

TEST 207A

Grid= 5.00000 Km

No Features Detected

Grid= 20.0000 Km

Feature # 1 Top= 4.800 Km Base= 0.990 Km

Parameter	Min	Max	Mean	StDev	Target
532 Lidar Ratio	19.7501	23.7624	21.7193	1.0666	21.9790
064 Lidar Ratio	31.3720	31.3720	31.3720	0.0000	31.3720
532 Optical Depth	0.1710	0.1710	0.1710	0.0000	0.1710
064 Optical Depth	0.1822	0.2043	0.1937	0.0055	0.1960
532 Ext Coeff	-0.0141	0.1064	0.0445	0.0161	0.0450
064 Ext Coeff	-0.0045	0.0778	0.0506	0.0100	0.0515
532 Backscatter	-5.97e-04	4.82e-03	2.05e-03	7.46e-04	2.05e-03
064 Backscatter	-1.43e-04	2.48e-03	1.61e-03	3.18e-04	1.64e-03
532 Color Ratio	0.8197	1.2203	0.9509	0.0990	0.8020
532 Vert Ext SD	0.0133	0.0185			
064 Vert Ext SD	0.0082	0.0112			
532 Horz Ext SD	0.0090	0.0275			
064 Horz Ext SD	0.0053	0.0127			

Grid= 80.0000 Km

No Features Detected

Table A9. Simulation Case 208B.

TEST 208B

Grid= 5.00000 Km

Feature # 1 Top= 2.490 Km Base= 0.990 Km

Parameter	Min	Max	Mean	StDev	Target
532 Lidar Ratio	37.1910	37.1910	37.1910	0.0000	37.1910
064 Lidar Ratio	34.8820	34.8820	34.8820	0.0000	34.8820
532 Optical Depth	0.1444	0.2291	0.1880	0.0170	0.1888
064 Optical Depth	0.0919	0.1256	0.1116	0.0063	0.1130
532 Ext Coeff	0.0089	0.3298	0.1229	0.0396	0.1250
064 Ext Coeff	0.0033	0.1339	0.0739	0.0165	0.0755
532 Backscatter	2.41e-04	8.87e-03	3.30e-03	1.06e-03	3.36e-03
064 Backscatter	9.39e-05	3.84e-03	2.12e-03	4.72e-04	2.16e-03
532 Color Ratio	0.5749	1.0847	0.7283	0.0965	0.6440
532 Vert Ext SD	0.0135	0.0276			
064 Vert Ext SD	0.0084	0.0144			
532 Horz Ext SD	0.0334	0.0467			
064 Horz Ext SD	0.0129	0.0183			

Feature # 2 Top= 4.800 Km Base= 2.490 Km

Parameter	Min	Max	Mean	StDev	Target
532 Lidar Ratio	21.9790	21.9790	21.9790	0.0000	21.9790
064 Lidar Ratio	31.3720	31.3720	31.3720	0.0000	31.3720
532 Optical Depth	0.0868	0.1294	0.1021	0.0075	0.1040
064 Optical Depth	0.1065	0.1327	0.1190	0.0055	0.1180
532 Ext Coeff	-0.0040	0.2201	0.0452	0.0193	0.0450
064 Ext Coeff	-0.0077	0.1013	0.0514	0.0117	0.0515
532 Backscatter	-1.83e-04	5.92e-03	2.01e-03	7.46e-04	2.05e-03
064 Backscatter	-2.45e-04	2.94e-03	1.64e-03	3.67e-04	1.64e-03
532 Color Ratio	0.6926	2.1587	0.9974	0.1678	0.8000
532 Vert Ext SD	0.0135	0.0276			
064 Vert Ext SD	0.0084	0.0144			
532 Horz Ext SD	0.0118	0.0355			
064 Horz Ext SD	0.0087	0.0139			

(Continued next page)

Grid= 20.0000 Km

Feature # 1 Top= 0.990 Km Base= 0.030 Km

Parameter	Min	Max	Mean	StDev	Target
532 Lidar Ratio	60.9000	60.9000	60.9000	0.0000	60.9000
064 Lidar Ratio	45.9000	45.9000	45.9000	0.0000	45.9000
532 Optical Depth	0.0258	0.0506	0.0363	0.0063	0.0800
064 Optical Depth	0.0081	0.0157	0.0128	0.0019	0.0240
532 Ext Coeff	-0.0245	0.1200	0.0372	0.0236	0.0800
064 Ext Coeff	-0.0070	0.0348	0.0136	0.0076	0.0240
532 Backscatter	-4.02e-04	1.97e-03	6.10e-04	3.87e-04	1.31e-03
064 Backscatter	-1.52e-04	7.59e-04	2.96e-04	1.66e-04	5.23e-04
532 Color Ratio	11424.8193	undef.	undef.	2866.7485	0.3992
532 Vert Ext SD	0.0176	0.0281			
064 Vert Ext SD	0.0047	0.0105			
532 Horz Ext SD	0.0000	0.0285			
064 Horz Ext SD	0.0000	0.0084			

Grid= 80.0000 Km

No Features Detected

Table A10. Simulation Case 209B.

TEST 209B

Grid= 5.00000 Km

No Features Detected

Grid= 20.0000 Km

Feature # 1 Top= 2.490 Km Base= 0.990 Km

Parameter	Min	Max	Mean	StDev	Target
532 Lidar Ratio	37.1910	37.1910	37.1910	0.0000	37.1910
064 Lidar Ratio	34.8820	34.8820	34.8820	0.0000	34.8820
532 Optical Depth	0.1531	0.2247	0.1884	0.0192	0.1888
064 Optical Depth	0.1023	0.1279	0.1128	0.0066	0.1130
532 Ext Coeff	-0.0397	0.2677	0.1232	0.0473	0.1250
064 Ext Coeff	0.0029	0.1246	0.0748	0.0148	0.0755
532 Backscatter	-1.07e-03	7.20e-03	3.31e-03	1.27e-03	3.36e-03
064 Backscatter	8.26e-05	3.57e-03	2.14e-03	4.25e-04	2.16e-03
532 Color Ratio	0.5537	1.1267	0.7913	0.1407	0.6440
532 Vert Ext SD	0.0166	0.0317			
064 Vert Ext SD	0.0090	0.0132			
532 Horz Ext SD	0.0273	0.0663			
064 Horz Ext SD	0.0098	0.0174			

Feature # 2 Top= 4.800 Km Base= 2.490 Km

Parameter	Min	Max	Mean	StDev	Target
532 Lidar Ratio	21.9790	21.9790	21.9790	0.0000	21.9790
064 Lidar Ratio	31.3720	31.3720	31.3720	0.0000	31.3720
532 Optical Depth	0.0853	0.1245	0.1018	0.0099	0.1040
064 Optical Depth	0.1110	0.1263	0.1186	0.0049	0.1180
532 Ext Coeff	-0.0220	0.2115	0.0450	0.0219	0.0450
064 Ext Coeff	-0.0056	0.1058	0.0513	0.0110	0.0515
532 Backscatter	-1.00e-03	5.69e-03	2.00e-03	8.76e-04	2.05e-03
064 Backscatter	-1.80e-04	3.03e-03	1.63e-03	3.46e-04	1.64e-03
532 Color Ratio	0.7612	5.1465	1.3575	0.9080	0.8000
532 Vert Ext SD	0.0166	0.0317			
064 Vert Ext SD	0.0090	0.0132			
532 Horz Ext SD	0.0113	0.0457			
064 Horz Ext SD	0.0068	0.0135			

(Continued next page)

Grid= 80.0000 Km

Feature # 1 Top= 0.990 Km Base= 0.030 Km

Parameter	Min	Max	Mean	StDev	Target
532 Lidar Ratio	60.9000	60.9000	60.9000	0.0000	60.9000
064 Lidar Ratio	45.9000	45.9000	45.9000	0.0000	45.9000
532 Optical Depth	0.0308	0.0589	0.0423	0.0094	0.0800
064 Optical Depth	0.0114	0.0165	0.0140	0.0018	0.0240
532 Ext Coeff	-0.1812	0.8019	0.0465	0.0676	0.0800
064 Ext Coeff	-0.0085	0.0358	0.0148	0.0082	0.0240
532 Backscatter	-2.98e-03	1.32e-02	7.63e-04	1.11e-03	1.31e-03
064 Backscatter	-1.84e-04	7.79e-04	3.23e-04	1.79e-04	5.23e-04
532 Color Ratio	0.4626	undef.	undef.	9673.6104	0.3992
532 Vert Ext SD	0.0197	0.1414			
064 Vert Ext SD	0.0061	0.0103			
532 Horz Ext SD	0.0000	0.3074			
064 Horz Ext SD	0.0000	0.0108			

Table A11. Simulation Case 210A.

TEST 210A

Grid= 5.00000 Km

No Features Detected

Grid= 20.0000 Km

Feature # 1 Top= 1.500 Km Base= 0.030 Km

Parameter	Min	Max	Mean	StDev	Target
532 Lidar Ratio	40.2890	40.2890	40.2890	0.0000	40.2890
064 Lidar Ratio	27.2590	27.2590	27.2590	0.0000	27.2590
532 Optical Depth	0.0631	0.0817	0.0723	0.0042	0.0750
064 Optical Depth	0.0186	0.0247	0.0219	0.0015	0.0231
532 Ext Coeff	0.0000	0.1047	0.0487	0.0157	0.0500
064 Ext Coeff	-0.0043	0.0267	0.0148	0.0049	0.0152
532 Backscatter	0.00e+00	2.60e-03	1.21e-03	3.89e-04	1.24e-03
064 Backscatter	-1.58e-04	9.78e-04	5.43e-04	1.79e-04	5.58e-04
532 Color Ratio	0.3715	0.6440	0.4922	0.0490	0.4500
532 Vert Ext SD	0.0127	0.0186			
064 Vert Ext SD	0.0038	0.0061			
532 Horz Ext SD	0.0000	0.0181			
064 Horz Ext SD	0.0000	0.0056			

Grid= 80.0000 Km

No Features Detected

Table A12. Simulation Case 211A.

TEST 211A

Grid= 5.00000 Km

No Features Detected

Grid= 20.0000 Km

No Features Detected

Grid= 80.0000 Km

Feature # 1 Top= 1.500 Km Base= 0.030 Km

Parameter	Min	Max	Mean	StDev	Target
532 Lidar Ratio	40.2890	40.2890	40.2890	0.0000	40.2890
064 Lidar Ratio	27.2590	27.2590	27.2590	0.0000	27.2590
532 Optical Depth	0.0651	0.0778	0.0713	0.0049	0.0750
064 Optical Depth	0.0199	0.0237	0.0214	0.0014	0.0231
532 Ext Coeff	-0.1502	0.1652	0.0479	0.0207	0.0500
064 Ext Coeff	-0.0038	0.0233	0.0145	0.0042	0.0152
532 Backscatter	-3.73e-03	4.10e-03	1.19e-03	5.14e-04	1.24e-03
064 Backscatter	-1.41e-04	8.54e-04	5.31e-04	1.56e-04	5.58e-04
532 Color Ratio	0.4164	0.5177	0.4608	0.0357	0.4500
532 Vert Ext SD	0.0139	0.0313			
064 Vert Ext SD	0.0035	0.0051			
532 Horz Ext SD	0.0000	0.1242			
064 Horz Ext SD	0.0000	0.0053			

Table A13. Simulation Case 212.

TEST 212

Grid= 5.00000 Km

Feature # 1 Top= 15.015 Km Base= 4.980 Km

Parameter	Min	Max	Mean	StDev	Target
532 Lidar Ratio	14.8500	15.0000	14.9937	0.0301	15.0000
064 Lidar Ratio	15.0000	15.0000	15.0000	0.0000	15.0000
532 Optical Depth	1.1663	3.8213	1.7235	0.3539	12.0000
064 Optical Depth	1.2633	2.1490	1.5818	0.1461	12.0000
532 Ext Coeff	-0.3028	4.8102	0.1266	0.3296	1.2000
064 Ext Coeff	-0.5019	1.1753	0.1185	0.3087	1.2000
532 Backscatter	-2.02e-02	3.21e-01	8.45e-03	2.20e-02	
064 Backscatter	-3.35e-02	7.84e-02	7.90e-03	2.06e-02	
532 Color Ratio	0.5297	47.3018	2.7594	4.8670	1.0000
532 Vert Ext SD	0.2490	0.8611			
064 Vert Ext SD	0.2781	0.3450			
532 Horz Ext SD	0.0087	0.4909			
064 Horz Ext SD	0.0046	0.1536			

Grid= 20.0000 Km

No Features Detected

Grid= 80.0000 Km

No Features Detected

Table A14. Simulation Case 213.

TEST 213

Grid= 5.00000 Km

Feature # 1 Top= 15.015 Km Base= 4.980 Km

Parameter	Min	Max	Mean	StDev	Target
532 Lidar Ratio	13.7028	15.0000	14.8386	0.2744	15.0000
064 Lidar Ratio	14.7015	15.0000	14.9922	0.0398	15.0000
532 Optical Depth	0.9127	2.9780	1.6183	0.4666	12.0000
064 Optical Depth	1.2753	2.5405	1.6784	0.2911	12.0000
532 Ext Coeff	-22.1989	17.0610	0.1236	0.9309	1.2000
064 Ext Coeff	-5.7793	8.0417	0.1283	0.4331	1.2000
532 Backscatter	-1.53e+00	1.15e+00	8.37e-03	6.31e-02	
064 Backscatter	-3.85e-01	5.36e-01	8.56e-03	2.89e-02	
532 Color Ratio	0.5977	26.8891	2.9224	3.5969	1.0000
532 Vert Ext SD	0.2990	3.3092			
064 Vert Ext SD	0.3001	1.4971			
532 Horz Ext SD	0.0208	3.1177			
064 Horz Ext SD	0.0090	0.8779			

Grid= 20.0000 Km

No Features Detected

Grid= 80.0000 Km

No Features Detected